



Slowing down fat digestion and absorption by an oxadiazolone inhibitor targeting selectively gastric lipolysis

Vanessa Point, Anaïs Benarouche, Julie Zarrillo, Alexandre Guy, Romain Magnez, Laurence Fonseca, Brigitte Raux, Julien Leclaire, Gérard Buono, Frédéric Fotiadu, et al.

► To cite this version:

Vanessa Point, Anaïs Benarouche, Julie Zarrillo, Alexandre Guy, Romain Magnez, et al.. Slowing down fat digestion and absorption by an oxadiazolone inhibitor targeting selectively gastric lipolysis. European Journal of Medicinal Chemistry, 2016, 123 (834-848), 10.1016/j.ejmech.2016.08.009 . hal-01466841

HAL Id: hal-01466841

<https://hal.science/hal-01466841>

Submitted on 6 Dec 2022

HAL is a multi-disciplinary open access archive for the deposit and dissemination of scientific research documents, whether they are published or not. The documents may come from teaching and research institutions in France or abroad, or from public or private research centers.

L'archive ouverte pluridisciplinaire **HAL**, est destinée au dépôt et à la diffusion de documents scientifiques de niveau recherche, publiés ou non, émanant des établissements d'enseignement et de recherche français ou étrangers, des laboratoires publics ou privés.



Distributed under a Creative Commons Attribution - NonCommercial - NoDerivatives 4.0 International License

1 **Slowing down fat digestion and absorption by an oxadiazolone inhibitor**
2 **targeting selectively gastric lipolysis.**

3 Vanessa Point¹, Anais Bénarouche¹, Julie Zarrillo¹, Alexandre Guy³, Romain Magnez⁴,
4 Laurence Fonseca⁴, Brigitte Raux¹, Julien Leclaire^{2‡}, Gérard Buono², Frédéric Fotiadu²,
5 Thierry Durand³, Frédéric Carrière¹, Carole Vaysse⁴, Leslie Couëdelo^{4,*} and Jean-François
6 Cavalier^{1,*}

7

8

9 ¹ Aix-Marseille Univ, CNRS, EIPN, Marseille, France.

10 ² Aix-Marseille Univ, CNRS, Centrale Marseille, ISM2, France.

11 ³ Institut des Biomolécules Max Mousseron (IBMM), UMR 5247 – CNRS – UM – ENSCM,
12 Faculté de Pharmacie, 15 avenue Charles Flahault, 34093 Montpellier Cedex 5, France.

13 ⁴ ITERG-ENMS, Université de Bordeaux, rue Léo Saignat, 33076 Bordeaux Cedex, France.

14

15 * **Corresponding authors.**

16 L. Couëdelo: E-mail: l.couedelo@iterg.com; Phone: +33 557 575 729.

17 J.-F. Cavalier: E-mail: jfcavalier@imm.cnrs.fr; Phone: +33 491 164 093.

18

19 [‡] Current address: CNRS, Université Claude Bernard Lyon 1, CPE Lyon, ICBMS UMR 5246,
20 43 bd du 11 Novembre 1918, 69622 Villeurbanne Cedex, France.

21

1 **Abbreviations:** AUC, area under the curve; DAG, diacylglycerol; DGL, dog gastric lipase;
2 FFA, free fatty acid; GPLRP2, guinea pig pancreatic lipase-related protein 2; *h*CEH, human
3 carboxyl ester hydrolase; HGL, human gastric lipase; HPJ, human pancreatic juice; HPL,
4 human pancreatic lipase; HSL, hormone-sensitive lipase; MAG, monoacylglycerol; O/W, oil
5 in water ; PPE, porcine pancreatic extracts; PPL, porcine pancreatic lipase; RLL, rat lingual
6 lipase; TAG, triacylglycerol; TC4, tributyrin; V_i , initial velocity ; x_i , inhibitor molar excess
7 related to 1 mole of enzyme; x_{I50} , inhibitor molar excess leading to 50% lipase inhibition.

8
9
10

1 **Abstract**

2 Based on a previous study and *in silico* molecular docking experiments, we have designed
3 and synthesized a new series of ten 5-Alkoxy-*N*-3-(3-PhenoxyPhenyl)-1,3,4-Oxadiazol-2(3*H*)-
4 one derivatives (**RmPPOX**). These molecules were further evaluated as selective and potent
5 inhibitors of mammalian digestive lipases: purified dog gastric lipase (DGL) and guinea pig
6 pancreatic lipase related protein 2 (GPLRP2), as well as porcine (PPL) and human (HPL)
7 pancreatic lipases contained in porcine pancreatic extracts (PPE) and human pancreatic juices
8 (HPJ), respectively. These compounds were found to strongly discriminate classical pancreatic
9 lipases (poorly inhibited) from gastric lipase (fully inhibited). Among them, the 5-(2-
10 (**Benzyl**oxy)ethoxy)-3-(3-PhenoxyPhenyl)-1,3,4-Oxadiazol-2(3*H*)-one (**BemPPOX**) was
11 identified as the most potent inhibitor of DGL, even more active than the FDA-approved drug
12 **Orlistat**. **BemPPOX** and **Orlistat** were further compared *in vitro* in the course of test meal
13 digestion, and *in vivo* with a mesenteric lymph duct cannulated rat model to evaluate their
14 respective impacts on fat absorption. While **Orlistat** inhibited both gastric and duodenal
15 lipolysis and drastically reduced fat absorption in rats, **BemPPOX** showed a specific action on
16 gastric lipolysis that slowed down the overall lipolysis process and led to a subsequent reduction
17 of around 55% of the intestinal absorption of fatty acids compared to controls. All these data
18 promote **BemPPOX** as a potent candidate to efficiently regulate the gastrointestinal lipolysis,
19 and to investigate its link with satiety mechanisms and therefore develop new strategies to “*fight*
20 *against obesity*”.

21

22 **Keywords:** digestive enzyme, enzyme inhibition, lipases, oxadiazolone, gastrointestinal
23 digestion, intestinal absorption, lymphatic lipids.

24

1 **1. Introduction**

2 Among food components, fat is a major vehicle for calories. Reducing its consumption or
3 absorption appears obvious in order to reduce body weight. In fact, it is recognized that our
4 modern western diet contains too much fat (around 100 g/day), which increases the risk factors
5 for metabolic diseases such as obesity [1]. This human pathology is globally the fifth major
6 cause of death and it has increasingly affected more individuals during the last decade. In 2014,
7 nearly 30% of the worldwide population was either overweight or obese, of which 18.4% of the
8 adults aged 15 years and over were obese in OECD countries (source:
9 <http://www.oecd.org/health/obesity-update.htm>). The reduction of food uptake is at the
10 forefront of the various strategies to fight against obesity, using both nutritional and
11 pharmacological approaches.

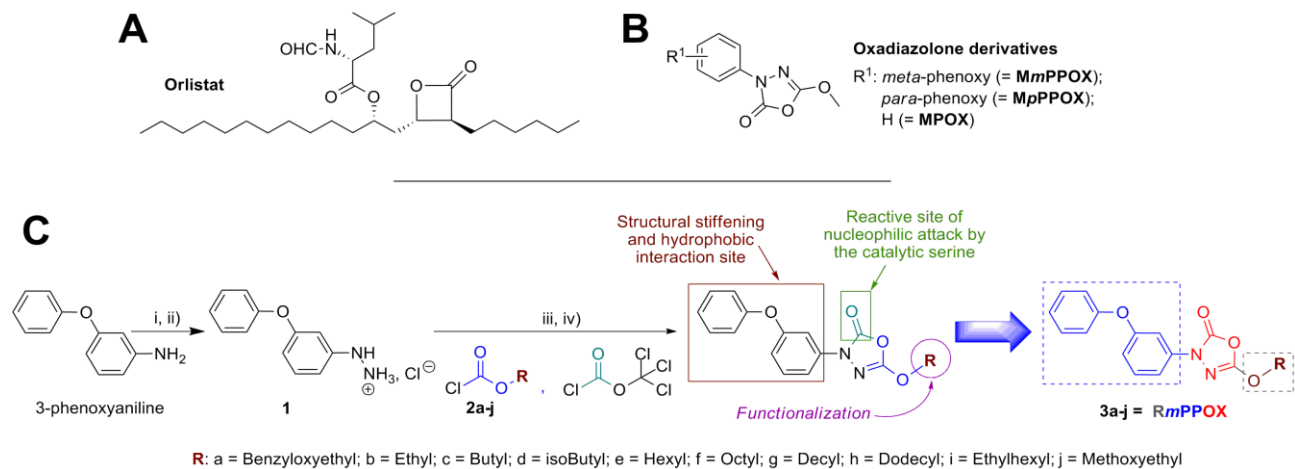
12 The inhibition of human digestive lipases (*i.e.*, human gastric (HGL) and pancreatic (HPL)
13 lipases) which reduces fat digestion and absorption has indeed become one of the main
14 pharmacological treatment of obesity [2]. Today, the major worldwide licensed anti-obesity
15 drug **Orlistat** (**Figure 1A**), found in Xenical® (*Roche*) and Alli® (*GlaxoSmithKline*), reduces
16 fat absorption by around 30-40%. This drug leads to moderate weight loss (around 10% in
17 patients with Body mass index, BMI>28; [3]) but significantly decreases risk factors such as
18 plasma lipid and glucose levels [4]. This is usually considered as an important step forward in
19 the absence of more efficient treatments. However, It is worth noting that cohort of patients
20 have regain weight during their second year of treatment by **Orlistat** without any explanation
21 being provided so far [3]. Moreover, classical nutritional approaches based on hypocaloric diets
22 also appear to be unsatisfactory, with weight regain often observed after the restrictive diet
23 period [5-7]. Taken together with the fact that **Orlistat** is also known to induce uncomfortable
24 side effects (such as diarrhea, fecal incontinence, abdominal pain... [8]), all these observations
25 currently preclude the launch on the market of more efficient drug formulations.

1 Blocking fat digestion may also have indirect side effects that have been underestimated
2 so far. Indeed, the products of fat digestion, mainly free fatty acids (FFA), play an essential role
3 in controlling the gut physiology [9, 10]. Overall, the release of FFA by digestive lipases
4 triggers biliary and pancreatic secretions through the release of cholecystokinin (CCK) [11, 12].
5 Conversely, FFA have a major role in the release of satiety hormones when they reach the distal
6 part of the small intestine and trigger the secretion of satiety gut hormones (*i.e.*, glucagon-like
7 peptide-1, GLP-1; peptide YY, PYY) [13] and the so-called “ileal brake” of food uptake [14].

8 The digestion of dietary fat (>95% triacylglycerols (TAG)) is a complex and dynamic
9 process which starts in the upper gastrointestinal (GI) tract under the action of HGL in humans,
10 and is completed in the small intestine by HPL [15, 16]. Although HGL only contributes to one
11 fourth of the lipolysis process yielding absorbable digestion products (FFA and
12 monoacylglycerols (MAG)), this lipase plays an important role in triggering the subsequent
13 action of HPL [17-19], as well as in the early release of short (SCFA) and medium (MCFA)
14 chain fatty acids that can be directly absorbed by the stomach mucosa (<C12) [20-22]. At this
15 stage, gastric lipolysis induces a critical modification of the lipid/water interface of emulsified
16 TAGs and promotes the activity of pancreatic lipase in the intestine, thus reflecting the
17 synergistic action of these two lipases.

18

1



2

3

Fig. 1. Structure of (A) **Orlistat** and (B) oxadiazolone derivatives **MmPPOX**, **MpPPOX** and **MPOX** initially tested on digestive lipases [23]. (C) General procedure for the one step preparation of 5-alkoxy-3-(3-phenoxyphenyl)-1,3,4-oxadiazol-2(3*H*)-one compounds (**3a-j** = **RmPPOX**) from 3-phenoxy-phenylhydrazine (**1**). *Reagents and conditions:* i) NaNO₂, HCl, 0 °C; ii) SnCl₂, HCl, 0°C, 73–81%; iii) Alkyl chloroformate **2a-j**, Pyridine, 0 °C to RT; iv) ClCO₂CCl₃, CHCl₂, Pyridine, 0 °C to RT, 38–50%.

4

In the context of “*fight against obesity*”, the search for new specific inhibitors of digestive lipases leading to potential anti-obesity drugs with low secondary effects represents a real challenge in a very competitive context. Recently we have identified that oxadiazolone compounds 5-**Methoxy-N-3-Phenyl** substituted-1,3,4-**Oxadiazol-2(3*H*)-ones** (namely: **MPOX**, as well as the ***meta*** and ***para*-PhenoxyPhenyl** derivatives, *i.e.* **MmPPOX** and **MpPPOX** – **Figure 1B**) were selective inhibitors of HGL with higher potency than **Orlistat**, but without any significant impact on the lipolytic activity of HPL [23]. We have also demonstrated in this work that the phenoxy group played a crucial role in specific molecular interactions at the gastric lipase’s active site. Its absence clearly impaired the inhibitory power exerted by **MPOX**, while its presence in the case of **MmPPOX** and **MpPPOX** led to a significant gain in selectivity and potency. The use of such compounds specifically designed to block gastric lipase while leaving pancreatic lipase activity unaffected, should allow to better investigate the individual effects of each digestive lipase on the overall lipolysis process. While pathological situations

1 of pancreatic lipase deficiency are known and have allowed to study the contribution of gastric
2 lipase alone [24], there is no equivalent situation for gastric lipase known so far. Shutting down
3 gastric lipolysis is expecting to slow down the overall lipolysis process, with an impact on the
4 rate of intestinal absorption of lipids.

5 In this perspective and taking into accounts the structural basis for the specific inhibition
6 of our target enzymes by this family of oxadiazolone compounds, as revealed by *in silico*
7 docking experiments [23], a new series of lipophilic inhibitors based on an oxadiazolone-core
8 (**Figure 1C**) has been synthesized and tested on various mammalian digestive lipases. The
9 (*meta*-phenoxy)phenyl group, responsible for strong hydrophobic interactions and structural
10 stiffening [23], was conserved in all new candidate inhibitors. In addition, modifying the **R**
11 chain born by the oxadiazolone ring will allow to investigate the influence of the lipophilicity
12 on the inhibitory power exerted by these molecules towards our target enzymes. Indeed, such
13 side **R** chain is anticipated either to be buried in hydrophobic clefts around the active site or to
14 point towards the surface of the protein, therefore leading to an expected improvement in
15 inhibition level and selectivity against DGL and/or HPL. The most potent inhibitor identified
16 was further used both in the *in vitro* simulation of GI lipolysis [2, 25], and *in vivo* using an
17 experimental animal model (*i.e.*, rat [26, 27]).

18

19 **2. Results & Discussion**

20 *2.1. Chemistry.*

21 Based on the chemical structure of **MmPPOX**, a new series of oxadiazolone derivatives
22 was designed by keeping the phenoxy group in *meta* position on the aromatic ring and by
23 varying the nature of the **R** chain on the oxadiazolone moiety (**Figure 1C**). The synthesis of
24 these 5-alkoxy-3-(3-phenoxyphenyl)-1,3,4-oxadiazol-2(3H)-one compounds (**3a-j**), was
25 carried out from commercial 3-phenoxyaniline as previously described [23]. For *in vivo* study
26 purposes, this initial procedure was however optimized and scaled-up to multi-grams by

1 performing both the coupling reaction with alkyl chloroformate **2a-j** (step *iii*) and the
2 cyclization reaction with diphosgene (step *iv*) in a one-pot two-steps reaction. In that way, ten
3 new lipophilic oxadiazolone derivatives were synthesized with good overall yields ranging
4 from 38 to 50% depending on the nature of the alkyl chain **R**, and purity ($\geq 97\%$ as determined
5 by HPLC analysis). To remain consistent with the names of the previous compounds [23], we
6 have developed a specific nomenclature for these derivatives noted **RmPPOX**; where **mPP**
7 represents the *meta*-PhenoxyPhenyl group; **OX** the Oxadiazolone core; and **R** the alkyl chain
8 (*i.e.*, **B_e**, benzyloxyethyl; **E**, ethyl ; **B**, butyl ; **iB**, isobutyl ; **H**, hexyl ; **O**, octyl ; **Eh**, ethylhexyl ;
9 **D**, decyl ; **D_o**, dodecyl ; **M_e**, methoxyethyl).

10

11 *2.2. In vitro inhibition of digestive lipases by oxadiazolone compounds as compared to Orlistat.*

12 The new oxadiazolone **RmPPOX** derivatives were further tested for their inhibitory
13 activity towards mammalian digestive lipases: human (HPL) and porcine (PPL) pancreatic
14 lipases (contained in human pancreatic juices (HPJ) and porcine pancreatic extracts (PPE),
15 respectively); dog gastric lipase (DGL) which provides a good model for HGL [28-30]; and
16 guinea pig pancreatic lipase-related protein 2 (GPLRP2). GPLRP2 belongs to the pancreatic
17 lipase gene family [31], but the lid domain which controls the access to the active site in HPL,
18 is missing in GPLRP2 therefore providing this enzyme with unusual kinetic and inhibition
19 properties [32-34]. The pH-stat technique [23, 35] was used to measure lipase activities and
20 quantify the inhibitory power, defined here as the inhibitor molar excess leading to 50% lipase
21 inhibition (x_{150} value) [23, 36]. Thereby, a x_{150} value of 0.5 is synonymous with a 1:1
22 stoichiometric ratio between the inhibitor and the lipase and is therefore the highest level of
23 inhibitory activity that can be achieved.

24 As in the case of our first experiments involving **MmPPOX** derivatives [23], the weakest
25 inhibition was observed on porcine and human pancreatic lipases (**Table 1**). The enzyme
26 activity of both PPE and HPJ was indeed poorly reduced by around 13.2% to 32.5% in the

1 presence of the oxadiazolone inhibitors and at a very high inhibitor molar excess ($x_I = 400$).
2 Increasing the time of incubation up to 120 min did not improve the level of inhibition.
3 **MmPPOX** seems to be the sole oxadiazolone compound able to efficiently inhibit the porcine
4 pancreatic lipase (89.7% inhibition) with a moderate impact on human pancreatic lipase (43-
5 49% inhibition) (**Table 1**) [23].

6 A significant level of inhibition was however obtained on DGL and GPLRP2 (**Table 1**).
7 These two digestive lipases were strongly inactivated by most of the oxadiazolone compounds,
8 and the efficiency of the inhibition was found to depend on the chemical structure of each
9 inhibitor, and more precisely on the nature of the **R** group (**Table 1**). **DomPPOX** and
10 **EhmPPOX** exhibited very low inhibitory effects towards DGL, with 27% and 38% inhibition
11 at a high x_I value of 20, respectively (**Table 1**). In all other cases, x_{I50} values were indicative
12 either of a poor ($x_{I50} = 11.8$ for **MemPPOX**), medium (mean $x_{I50} = 5.07 \pm 0.6$ for **EmPPOX**,
13 **BmPPOX**, **iBmPPOX**, **HmPPOX**, **OmPPOX** and **DmPPOX**) or very potent ($x_{I50} = 0.50$ for
14 **BemPPOX**) inhibition. In the latter case, treating DGL with **BemPPOX** resulted in the
15 strongest inhibition of this enzyme, even at low x_I values (nearly 90% inhibition at $x_I = 4$), with
16 formation of a covalent 1:1 stoichiometric complex ($x_{I50} = 0.50$).

17 Regarding GPLRP2, low lipophilic compounds such as **EmPPOX** and **BmPPOX** bearing
18 respectively a short ethyl and butyl alkyl chain, exhibited rather weak inhibitory power with
19 x_{I50} values above 40 (*i.e.*, 27.7% and 43.8% inhibition, respectively, at high molar excess $x_I =$
20 20). In contrast, the other oxadiazolone derivatives strongly inhibited GPLRP2 with x_{I50} values
21 in the 0.52 to 2.80 range, corresponding to 48% to 90% inhibition at $x_I = 4$. Among them,
22 **HmPPOX** bearing a medium hexyl chain length can be considered as the best inhibitor of
23 GPLRP2 with >90% inhibition at $x_I = 4$ and a x_{I50} value of 1.09. It is worth mentioning that
24 **BemPPOX** is also a rather good inhibitor of GPLRP2 ($x_{I50} = 0.64$), but this compound led to a
25 maximum inhibition value of only 62.7% at high $x_I = 20$. **BemPPOX** may therefore inhibit the
26 homologous human and rat enzymes [37, 38], but this possibility was not tested here.

1 From all these data, no clear trends or rules in terms of structure-activity relationships
2 (SAR) have however emerged regarding the potency and selectivity of these oxadiazolone-core
3 compounds. Indeed, increasing the lipophilicity by varying the nature of the **R** chain on the
4 oxadiazolone ring has unfortunately neither improved the selectivity nor the inhibitory power
5 of the obtained compounds towards pancreatic lipases; *i.e.*, PPL and HPL. With GPLRP2, the
6 good inhibition reached with the derivatives bearing medium to long alkyl **R** chains length is
7 consistent with the broad range of substrates hydrolyzed by this lipase [39-41]. Concerning
8 gastric lipase, among all oxadiazolone compounds tested, the results obtained clearly revealed
9 the high inhibitory potency of **BemPPOX**, which acts stoichiometrically with DGL. Under
10 these conditions (lipase pre-incubation with inhibitor and bile salts before adding substrate and
11 measuring residual activity), this molecule is a more potent inhibitor than **Orlistat** (**Table 1**)
12 and it is in fact the most powerful inhibitor of gastric lipase identified so far.

13 Regarding the poor inhibitory effect of oxadiazolone compounds on lipases from PPE and
14 HPJ, it is noteworthy that these crude extracts of pancreatic enzymes contain classical
15 pancreatic lipase (PPL and HPL, respectively) but also carboxyl-ester hydrolase (CEH). CEH
16 is a non-specific esterase [42, 43] which accounts for 4% of the total proteins content of human
17 pancreatic juice [44], and contributes to overall gastro-intestinal lipolysis by hydrolyzing a
18 broad range of substrates [45]. Consequently, lipase activity measurements and inhibition tests
19 with PPE and HPJ simultaneously involved both classical pancreatic lipase and CEH [46, 47].
20 Although CEH specific activity on TAGs under pancreatic lipase assay conditions is two orders
21 of magnitude lower than the specific activity of pancreatic lipase [47], this prompted us to test
22 the effect of **BemPPOX** on CEH activity separately. Treating pure human CEH (*h*CEH) with
23 **BemPPOX** resulted in a strong inhibition of the lipase (71.5% inhibition at $x_I = 20$; $x_{I50} = 1.42$);
24 therefore suggesting that contrary to pancreatic lipase, the lipolytic activity of CEH present in
25 PPE or in HPJ would be fully inactivated by this oxadiazolone compound.

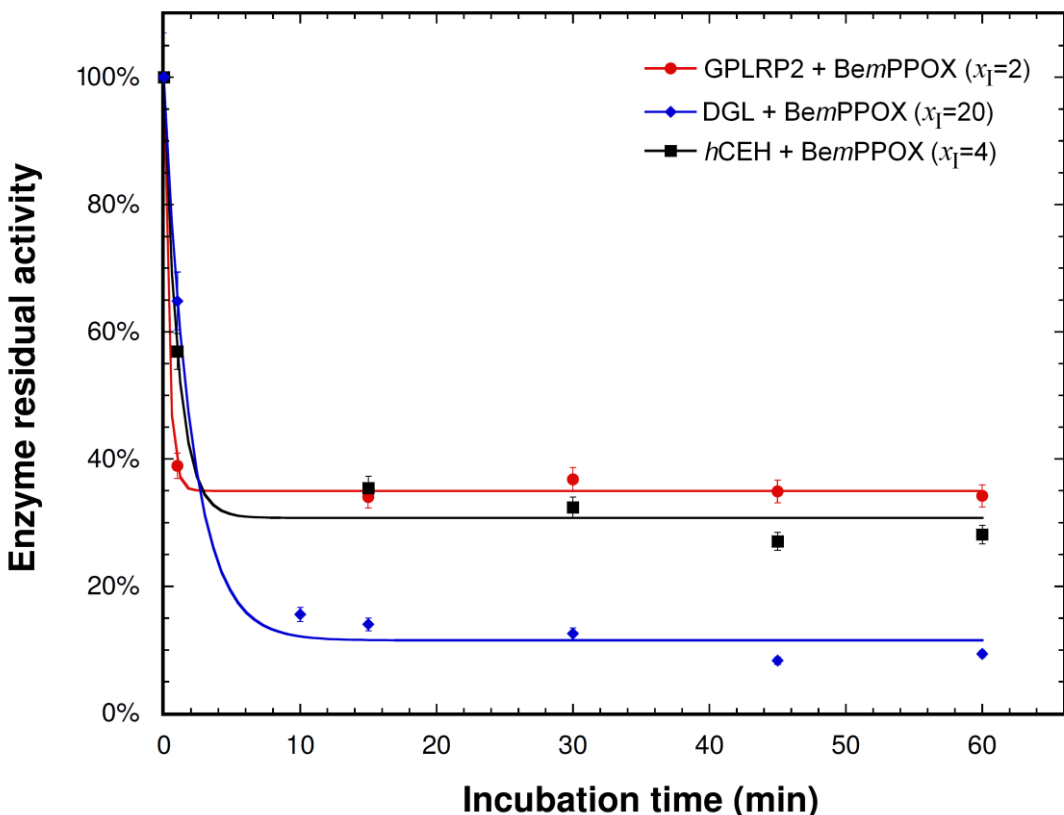


Fig. 2. Effect of the incubation time on the inhibition level of GPLRP2 (●), DGL (◆) and *hCEH* (■) by **BemPPOX**. Each enzyme was pre-incubated at a constant inhibitor molar excess ($x_I = 2, 20$ and 4 with GPLRP2, DGL and *hCEH*, respectively), and the residual activity was measured over a 60-min period at various time intervals using the pH-stat technique, as described in the Experimental section. Results are expressed as mean values \pm SD of at least three independent assays ($CV\% < 5.0\%$).

The influence of the incubation time on the levels of inhibition of GPLRP2, DGL and *hCEH* by **BemPPOX** was further investigated. As depicted on **Figure 2**, the residual activity of the three enzymes decreased sharply and reached a plateau value after approximately 15 min of incubation. From these inhibition curves, the values of the half-inactivation time ($t_{1/2}$) were deduced and found to be of 0.52 min, 1.68 min, and 1.31 min with GPLRP2, DGL and *hCEH*, respectively. The presence of an inhibition plateau reached with all three enzymes is not obvious to explain. This may result from the concomitant inhibition and partial reactivation of lipases since lipase inhibition by oxadiazolone compounds has been shown to be a reversible process [48].

Such low values of $t_{1/2}$, which reflect an extremely high rate of inhibition of each lipase by **BemPPOX**, were found to be of the same order of magnitude as those previously reported for **Orlistat** (**Supplementary data Table S1**) and **MnPPOX** on the same enzymes [23]. Moreover, the most significant results obtained are related not only to the inhibitory effect of **BemPPOX** which reaches similar levels on GPLRP2 and *hCEH* than those achieved with **Orlistat** ($x_{150} = 0.53$ and 0.78, respectively), but above all on the fact that this oxadiazolone compound exhibits a 11.2-fold higher potency on DGL than the aforementioned FDA-approved anti-obesity drug ($x_{150} = 5.60$) (**Supplementary data Table S1**).

9

10 2.3. *In silico* molecular docking.

To further investigate the interactions occurring at the lipases' active site during the binding of the oxadiazolone derivatives, *in silico* molecular docking experiments were conducted using the reported crystal structures of DGL (PDB code: 1K8Q [49]), GPLRP2-HPL chimera (PDB code: 1GPL [33]) and *hCEH* (PDB code: 1F6W [50]). In all cases, the best scoring positions obtained (*i.e.* lowest energy complex) showed that the reactive oxadiazolone ring adopted a productive orientation (**Figure 3 and Supplementary Data Figs S2-S3**). The reactive sp^2 carbon atom of the inhibitors carbonyl group was indeed found in a favorable position facilitating the occurrence of a reaction with the catalytic serine ($d[\text{Ser-Oy/C}_{\text{carb}}]$) distances $< 2.5 \text{ \AA}$) and thus the formation of a covalent bond. Moreover, all productive positions obtained with each oxadiazolone within DGL and GPLRP2 active site would be perfectly superimposed (**Figure 3B and Supplementary Data Fig. S2**).

More precisely, the open conformation of DGL, used as a reference model to check the reliability of the obtained oxadiazolone's docked positions, was corresponding to the one in which the *O*-butyl *n*-undecylphosphonate was covalently bound to the catalytic Ser¹⁵³ residue [49]. This receptor indeed appeared to be an optimal structure for *in silico* docking and to reliably depict the molecular interactions potentially involved with the best inhibitor within the

1 DGL active site. First, a high level of concordance between the most favorable docked
2 conformation of **BemPPOX** and the crystal structure of the covalently bound alkylphosphonate
3 was observed, therefore suggesting similar binding mode (**Figure 3C**). The docked **BemPPOX**-
4 DGL complex was then subjected to interactions analysis using Ligplot⁺ v.1.4 [51] (**Figure**
5 **3D**). The Ligplot+ diagram thereby generated schematically depicts the hydrogen bonds and
6 hydrophobic interactions between the ligand (*i.e.*, **BemPPOX**) and the active site residues of
7 the protein (*i.e.*, DGL) during the binding process. As depicted in **Figure 3D**, the Ligplot+
8 analysis clearly shows that, similarly to the covalent complex obtained with the phosphonate
9 inhibitor, the reactive *sp*² carbonyl atom of the oxadiazolone moiety is stabilized by H-bonding
10 with Gly¹⁵⁴ and Leu⁶⁷ residues forming the oxyanion hole. Moreover, twelve hydrophobic
11 contacts can be detected and appear critical to stabilize the **BemPPOX** side chains inside the
12 DGL active site (**Figure 3A&D**). The *meta*-phenoxyphenyl ring perfectly fits the hydrophobic
13 pocket opposite to the catalytic Ser¹⁵³ residue, and interacts with Val¹⁸², Val¹⁸⁵, Thr¹⁸⁸, Thr¹⁹⁰,
14 Trp²⁷⁵, Val²⁷⁹ and Leu³²⁶ residues. The 2-(benzyloxy)ethoxy group may point towards the
15 entrance of the active site thus interacting with Leu⁶⁸, Ile¹⁹², Met¹⁹⁶, Ile²⁴³ and Val²⁷² residues.

16 All these interactions therefore allow the formation of a stable and productive binding
17 mode, and provide a clear picture of the stoichiometric inhibition of gastric lipase by
18 **BemPPOX**.

19

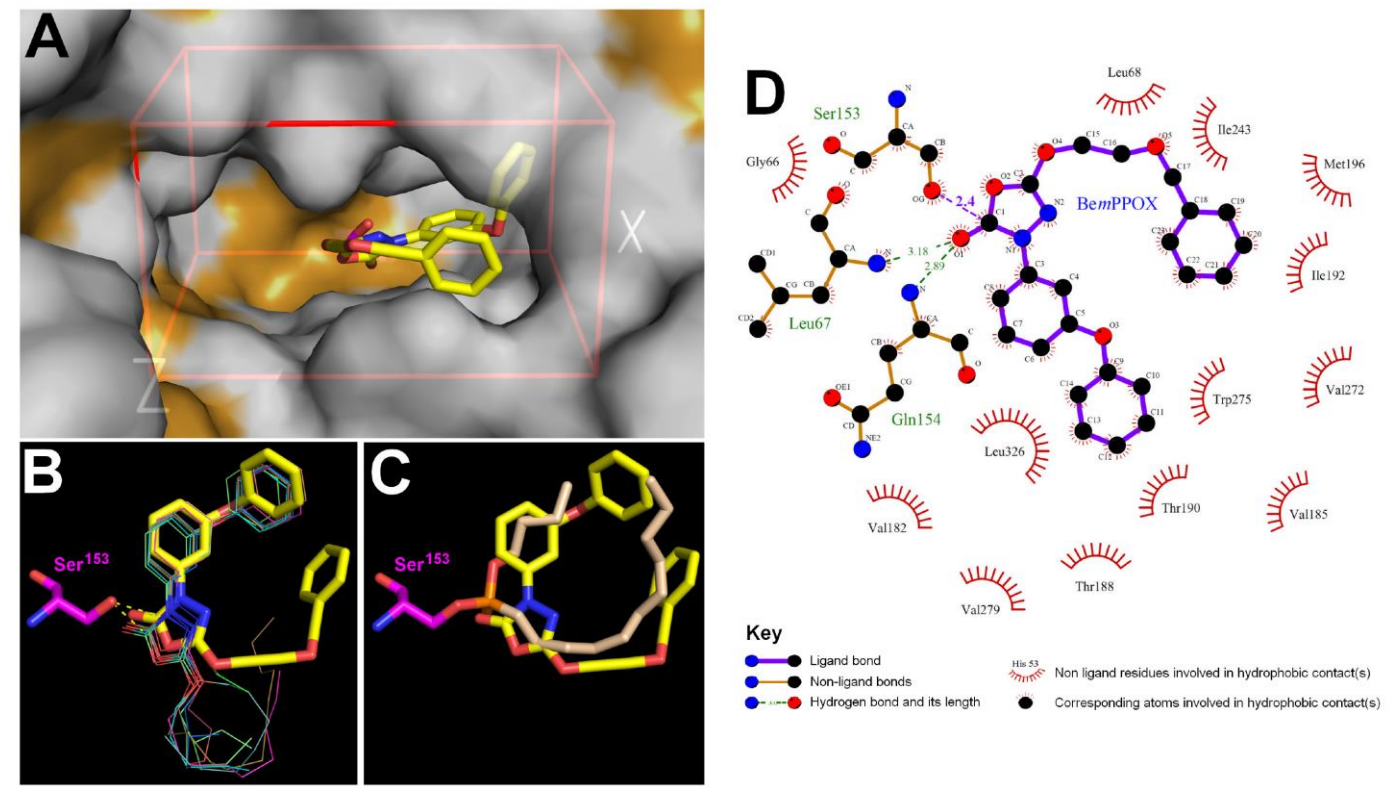


Fig. 3. (A) *In silico* molecular docking of **BemPPOX** into the crystallographic structure of DGL in a van der Waals surface representation. Hydrophobic residues (alanine, leucine, isoleucine, valine, tryptophan, tyrosine, phenylalanine, proline and methionine) are highlighted in white. **(B)** Superimposition of the top-scoring docking positions of the oxadiazolone inhibitors in DGL active site. **(C)** Superimposition of the top-scoring docking position of **BemPPOX** (yellow) with the crystal structure of covalently bound *O*-butyl *n*-undecylphosphonate (wheat) to the catalytic serine, as found in complex with DGL. **(D)** Ligplot+ analyses results: 2D representation of schematic ligand–protein interactions of **BemPPOX** in DGL active site showing both hydrogen-bond and hydrophobic interactions.

Each oxadiazolone inhibitor is represented in wireframe, **BemPPOX** and the covalently bound alkylphosphonate are in stick representation with the following atom color-code: nitrogen, blue; oxygen, red, phosphorus, orange. The catalytic Serine residue is colored in magenta. Structures were drawn with PyMOL Molecular Graphics System (Version 1.4, Schrödinger, LLC) using the PDB file: 1K8Q.

1

2 2.4. Assay of digestive lipase inhibition during *in vitro* gastrointestinal lipolysis of test meals.

3 The impact of **BemPPOX** on the hydrolysis of dietary lipids was further investigated with
4 *in vitro* simulation of gastrointestinal (GI) lipolysis taking into consideration both the gastric
5 and duodenal steps of digestion [2, 25]. In order to vary the nature and physicochemical
6 properties of the dietary TAGs, two different type of meals were used: a complete and pre-
7 emulsified liquid test meal (*i.e.*, *Ensure Plus*), and a solid test meal containing various
8 ingredients (grilled beef meat, French fries, string beans, butter and sunflower oil). This *in vitro*
9 digestion model has already been applied for studying the lipolysis of test meals containing
10 various fats [52], to predict the inhibitory power of **Orlistat** [2], to investigate the effects of
11 lipolysis on the solubility of hydrophobic drugs present in lipid-based formulations [29, 53], as
12 well as the lipolysis of various emulsions [54, 55].

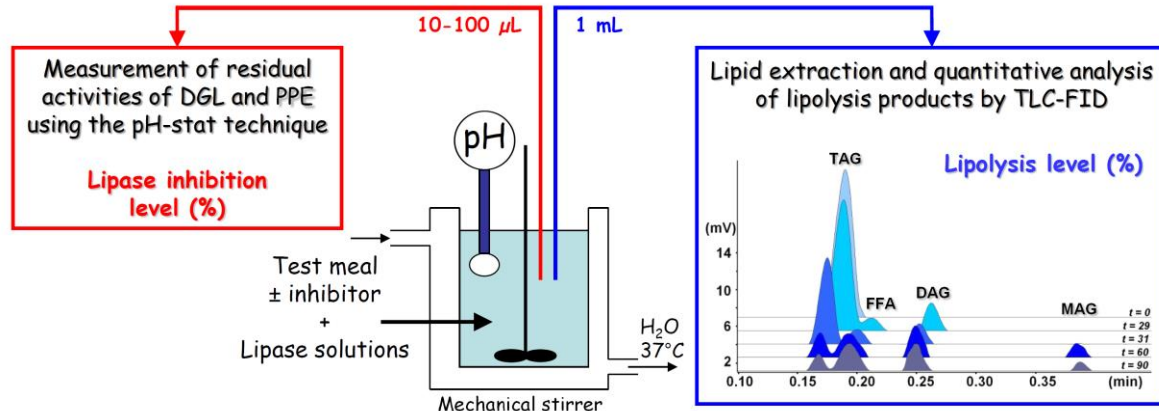
13 The liquid or solid test meal with or without inhibitor (**BemPPOX** or **Orlistat**) was first
14 mixed with a solution mimicking gastric juice and containing DGL for 30 min (*i.e.*, gastric step
15 of lipolysis) at pH 5.5. Then a solution mimicking pancreatic and bile secretions was added.
16 The resulting mixture was stirred for a further 60 min (*i.e.*, duodenal step of lipolysis) at pH
17 6.25. Commercially available PPE was used as a substitute of HPJ as often employed for *in*
18 *vitro* digestion studies [56-59].

19 With regards to the amount of inhibitor used, the meal volume-to-drug dose ratio was kept
20 identical to the ratio used for *in vivo* experiments (*i.e.*, 500-mL meal with 120 mg of the drug)
21 conducted with **Orlistat** [2]. For a 15-mL test meal, we used 3.6 mg of **Orlistat** as control
22 which corresponds to a molar excess of $x_1 = 1187$ with respect to DGL, and $x_1 = 66$ with respect
23 to PPL contained in PPE. To allow relevant comparison, this molar excess was kept constant
24 for both **BemPPOX** and **Orlistat**.

25 All along the *in vitro* digestion experiments in the presence/absence of **BemPPOX** or
26 **Orlistat**, residual lipase activities and lipolysis products resulting from lipolysis of test meal

1 TAGs were monitored by pH-stat measurements and TLC-FID analyses (**Figure 4**),
2 respectively [2, 25, 60].

3



4

5 **Fig. 4.** Scheme of the experimental device and assays performed in the course of *in vitro*
6 gastrointestinal digestion of a test meal. The chromatogram shows the typical evolution of the lipolysis
7 products during test meal TAG hydrolysis after extraction, separation and quantification of
8 triacylglycerols (TAG), free fatty acids (FFA), diacylglycerols (DAG), and monoacylglycerols (MAG)
9 by TLC-FID.

10

11 *2.4.1. In vitro lipolysis of test meals in control experiments.*

12 In the control experiments without inhibitor, we first checked that DGL and PPE activities
13 remained stable throughout the experiments with both the liquid (**Figure 5A**) and solid (**Figure**
14 **5C**) test meals. As previously observed [2], the lipolysis levels were found to be higher with
15 the liquid meal (**Figure 5B**) than with the solid meal (**Figure 5D**). With *Ensure Plus* liquid
16 meal, gastric lipolysis ($t = 0$ –29 min) reached a level of $22.3 \pm 1.4\%$ (**Figure 5B**) as compared
17 to $13.0 \pm 1.2\%$ (**Figure 5D**) with the solid meal. When PPE and bile were added ($t = 30$ min),
18 the lipolysis level of the liquid meal increased rapidly and reached a plateau value of around
19 $63.6 \pm 2.6\%$ at $t = 90$ min. By contrast, during the duodenal phase of digestion of the solid meal,
20 a slower increase in the level of lipolysis was observed from $15.7 \pm 0.7\%$ at $t = 31$ min to 45.4
21 $\pm 1.4\%$ at $t = 90$ min.

1 The rate of fat digestion is controlled by emulsions size and interfacial composition (*i.e.*
2 structure) of the lipids [61-63]. Here, the variation of +18.2% of the overall lipolysis level in
3 favor of the liquid *vs.* the solid meal, can thus be attributed to the respective physicochemical
4 state of the lipids in each test meal. In the liquid meal, the TAGs are pre-emulsified and
5 stabilized in the form of a fine emulsion by the phospholipids (*i.e.*, soy lecithin) present in the
6 *Ensure Plus*, therefore providing a good substrate for DGL and PPL. Conversely in the solid
7 meal, the physicochemical state of the lipids is more heterogeneous, and most of the TAGs have
8 to be emulsified in the course of the digestive process, thus leading to a lower rate of lipolysis
9 [52]. It is now well established that the presence and/or nature of surfactants and emulsifying
10 agents, commonly used in the human diet, differently impact the gastric and duodenal lipolysis
11 of lipid emulsions [64, 65]. Lecithin-stabilized emulsions provide an enhancing effect on
12 lipolysis regardless of oil or fat composition [54, 55]. For instance, we recently reported that
13 the emulsification of flaxseed oil with soya lecithin improved the gastric lipolysis of the oil
14 (+30%), while the presence of either Tween 80 or sodium caseinate strongly decreased it (-80%
15 and -40%, respectively) [55].

16

17 2.4.2. Effects of **BemPPOX** and **Orlistat** on *in vitro* lipolysis of test meals

18 In good agreement with the previous results on pure enzymes (**Table 1**), the activity of
19 DGL in the presence of the inhibitors was fully impaired at the end of the gastric phase of
20 digestion with both the liquid (**Figure 5A**) and solid (**Figure 5C**) meals. The rate of DGL
21 inhibition was found however to be slightly slower with **BemPPOX** than with **Orlistat** under
22 these conditions. Regarding PPE, and whatever the meal used, no significant inhibition was
23 obtained with **BemPPOX** (mean residual activity $94.7 \pm 1.2\%$), which contrasted with the high
24 86% level of inhibition induced by **Orlistat** (*i.e.*, mean residual activity $14.1 \pm 0.6\%$).

25 These lipase inhibition levels were further correlated to the corresponding lipolysis levels
26 (LL%) of test meal TAGs. Whatever the test meal used, gastric lipolysis was drastically reduced

1 in the presence of both lipase inhibitors (**Figure 5B&D; Table 2**). At $t = 29$ min, the lipolysis
2 level of the *Ensure Plus* meal was only $4.5 \pm 0.22\%$ (20.2% of control values) in presence of
3 **BemPPOX** and 0.0% with **Orlistat**. With the solid meal, similar and very low rates of lipolysis
4 in the 2.1-3.1% range (16.2-23.7% of control values) were obtained with both compounds
5 (**Table 2**).

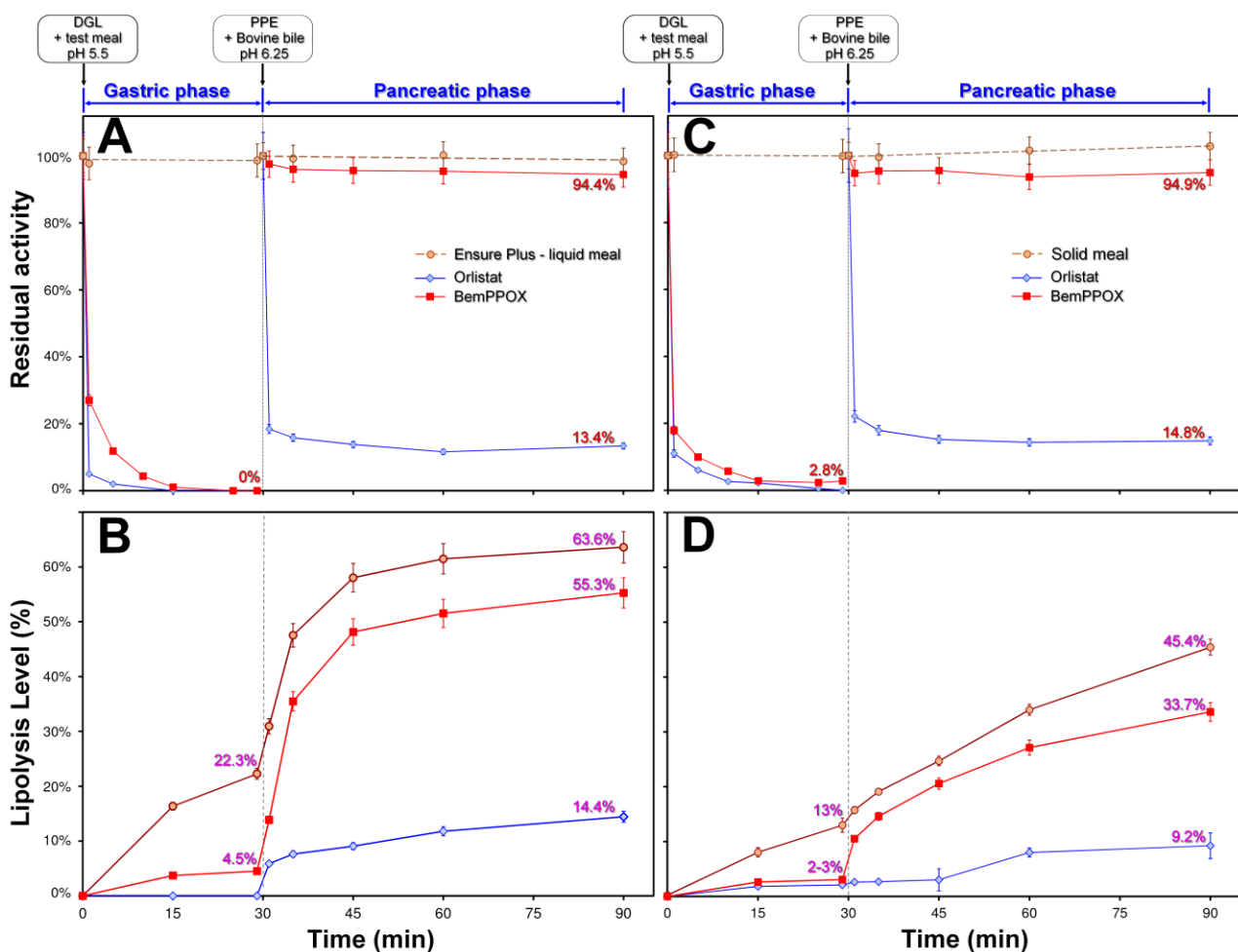
6 **Orlistat** also drastically reduced the duodenal phase of digestion by around 77-80%
7 (20.3-22.6% of control values at $t = 90$ min; **Table 2**) of both types of test meals and these data
8 correlated well with the low residual activities of DGL and PPE observed in the presence of
9 this inhibitor (**Figure 5A&C; Table 2**). When using **BemPPOX**, duodenal lipolysis of each
10 test meal increased rapidly after 15 min of incubation ($t = 45$ min; **Table 2**). The rate of lipolysis
11 then slowed down and reached at $t = 90$ min a maximum value of $55.3 \pm 2.6\%$ (86.9% of control
12 values) and $33.7 \pm 2.5\%$ (74.2% of control values) with the liquid and solid meals, respectively
13 (**Figure 5B&D; Table 2**). Interestingly, the difference of +21.6% in favor of the liquid *vs.* solid
14 meal in overall lipolysis level was similar to the one observed in control experiments (+18.2%,
15 see section 2.4.1).

16 With the *Ensure Plus* meal, the deviation between the lipolysis rates in presence and in
17 absence of **BemPPOX** at $t = 29$ min (-17.8%) was partly counterbalanced during the duodenal
18 step of lipolysis (+9.5% at $t = 90$ min). The contribution of pancreatic lipase to the overall
19 lipolysis level was indeed found to be 50.8% in the presence of **BemPPOX** as compared to
20 41.3% for control experiments. By contrast, when the solid meal was employed, no difference
21 in the contribution of pancreatic lipase was observed, with or without **BemPPOX** (31.6% *vs.*
22 32.4%, respectively). As a direct consequence, the observed deviation at $t = 29$ min (-10%)
23 was conserved at $t = 90$ min (LL% = 33.7% *vs.* 45.4% for controls).

24 *In vitro* digestion experiments mimicking the physiological gastrointestinal conditions
25 therefore confirmed **BemPPOX** specificity. This inhibitor drastically impairs the gastric step
26 of lipolysis regardless of the type of test meal, but had no significant effect on the rate of

1 duodenal lipolysis by pancreatic lipase, contrary to **Orlistat** which impairs both gastric and
 2 duodenal lipolysis. Moreover, we also demonstrated that the impact on the whole digestion
 3 process of the loss of gastric lipolysis is closely related to the physicochemical properties of the
 4 dietary TAGs [2].

5 The selective inhibition of the gastric lipase by **BemPPOX** in combination with the use of
 6 a solid meal, which is representative of a “normal” meal, allows to slow down the overall
 7 lipolysis process *in vitro* and suggests that this oxadiazolone inhibitor could be able to regulate
 8 the whole GI lipolysis *in vivo*.



9
 10 **Fig. 5.** Residual lipase activities (A and C) and lipolysis levels (B and D) during *in vitro*
 11 gastrointestinal digestion of liquid (A–B) and solid (C–D) test meals, in absence and presence of
 12 **BemPPOX** or **Orlistat**. Residual activities of DGL and PPL were measured during the gastric (0–30
 13 min) and duodenal (30–90 min) phases of digestion, respectively. Results are expressed as mean values
 14 ± SD of at least three independent assays (CV% < 5.0%).

1

2 2.5. Inhibition of the intestinal absorption of lipids in rats.

3 Based on *in vitro* data, the effects of **BemPPOX** vs. **Orlistat** on the intestinal absorption

4 of lipids were further assessed *in vivo* on rats. Rat is indeed a relevant animal model for studying

5 lipids absorption and to predict their metabolic fate in Humans. It is however worth noting that

6 the preduodenal lipase in rats is lingual and not gastric as in Humans [66, 67]. Rat lingual lipase

7 has however a similar contribution to TAGs digestion [67] and its inhibition should result in a

8 reduced gastrointestinal lipolysis and absorption of fat.

9 In this context, we firstly checked *in vitro* the inhibitory activity of both **BemPPOX** and

10 **Orlistat** on partly purified rat lingual lipase (RLL). As expected from the structural similarity

11 of RLL and gastric lipases [68, 69], both compounds strongly inactivated RLL activity

12 ($72.5 \pm 2.1\%$ mean inhibition at $x_1 = 4$) with x_{150} values of 1.43 and 0.70; respectively

13 (**Supplementary Data Table S1**).

14 With this prerequisite validated, the export kinetics of lipids (total TAG fatty acids) into

15 lymph compartment were followed over 24 hours in mesenteric lymph duct-cannulated rats

16 provided with the inhibitor compounds. Seven cannulated rats were used for each group: the

17 “*Control group*” only received olive oil emulsion, while the “*Orlistat group*” and the

18 “*BemPPOX group*” received olive oil emulsion supplemented with either **Orlistat** or

19 **BemPPOX** at a dose of 5.3 mg/kg of body weight.

20 The lipid secretion in lymph began from 2 to 3 hours after lipid administration rising to a

21 maximum concentration (C_{max}) at $t = 6$ h (*i.e.*, T_{max}) followed by a plateau phase, regardless of

22 the group (**Table 3 & Figure 6**). As expected, the lipid C_{max} in the *Orlistat group* (22.9 ± 3.0

23 mg/mL; *p-value* < 0.01) and in the *BemPPOX group* (33.6 ± 4.3 mg/mL; *p-value* = 0.04)

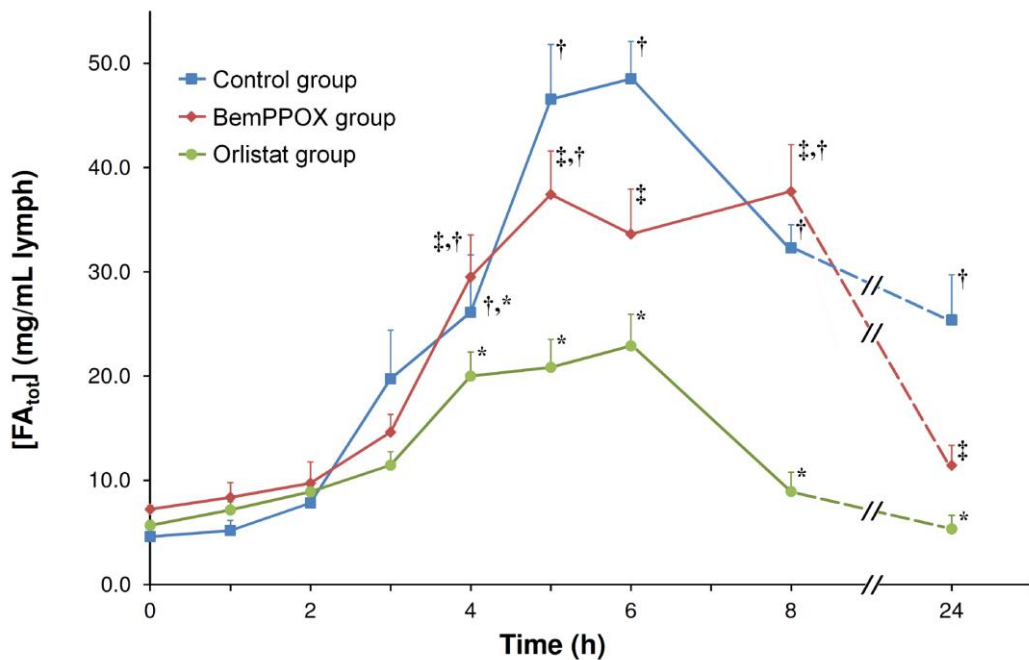
24 respectively amounted to 47% and 69% of the C_{max} value obtained in the *Control group*

25 (48.5 ± 3.6 mg/mL) (**Table 3**). Twenty four hours after gavage, the total fatty acid lymph

1 concentration in the *Orlistat group* (5.3 ± 1.3 mg/mL; $p\text{-value} = 0.01$) and in the *BemPPOX*
2 group (11.4 ± 1.9 mg/mL; $p\text{-value} = 0.02$) represented 21.0% and 45% of fatty acid
3 concentration in the *Control group* (25.4 ± 4.3 mg/mL).

4 The initial velocity (V_i) of lipid secretion in lymph, observed during the first hours of the
5 kinetics ($t = 2$ to 5 h), confirmed a slower lipid transition within the enterocytes when the
6 inhibitory compounds were used. In the *Orlistat group* the V_i value (4.4 ± 0.3 mg/mL/h) was
7 around two to three times lower than those observed in the *BemPPOX group* (9.8 ± 0.3
8 mg/mL/h) and in the *Control group* (12.3 ± 0.5 mg/mL/h), respectively (**Table 3**).

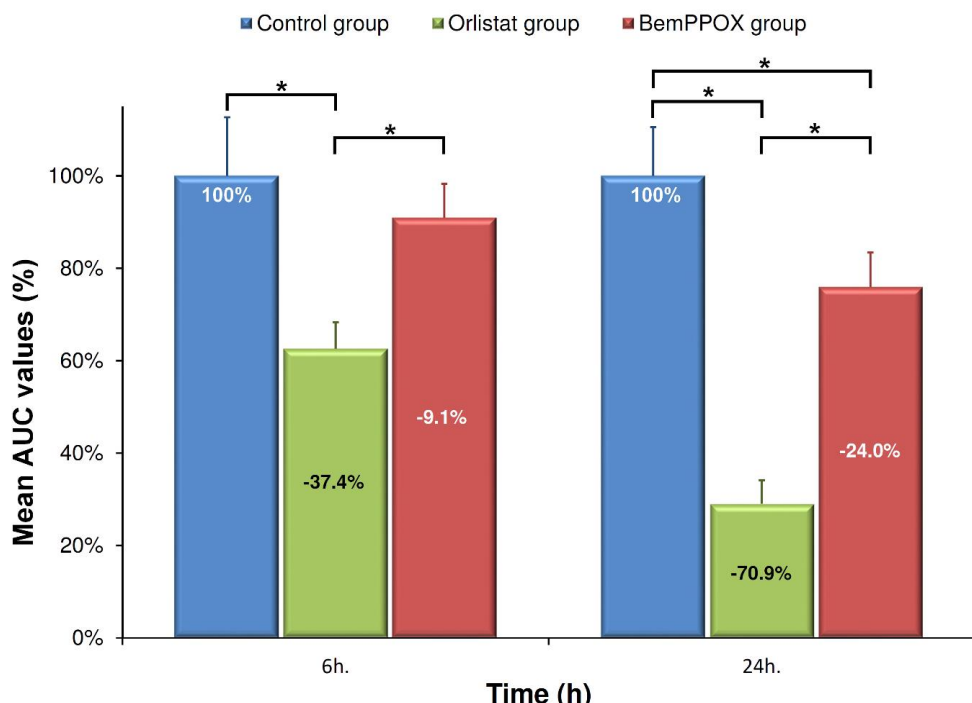
9



10
11 **Fig. 6.** Time course concentration of total fatty acids [FA_{tot}] in the lymph of rats fed with 0.8 mL
12 olive oil emulsion (*i.e.*, 530 mg fatty acids per rat) in *Control group* (■), or 0.8 mL olive oil emulsion
13 supplemented with either **BemPPOX** (◆) or **Orlistat** (●) at a dose of 5.3 mg/kg of body weight. Results
14 are expressed as mean values \pm SEM of at least 7 rats per group, at each time point. From $t = 3$ h, all
15 points differ significantly from the baseline. For a given time point, the [FA_{tot}] concentrations presented
16 without a common symbol (*, ‡, †) are significantly different ($p\text{-value} < 0.05$; ANOVA followed by
17 Fisher's test).

18

1 The experimental data obtained during the kinetics of lipid absorption allowed to further
 2 calculate the AUC (Area Under Curve) in order to estimate the overall fatty acid absorption,
 3 and by the way the *in vivo* efficacy of each inhibitor (**Figure 7 & Table 3**). At T_{max} time (*i.e.*, t
 4 = 6 h) the AUC confirmed the decrease in the overall lymphatic lipid absorption deduced from
 5 C_{max} values. The calculated AUC of the *Control group* ($132.0 \pm 16.7 \text{ h} \times \text{mg/mL}$) was indeed
 6 found to be reduced by 37.4% in the presence of **Orlistat** (AUC *Orlistat group* = 82.6 ± 7.6
 7 $\text{h} \times \text{mg/mL}$; $p\text{-value} = 0.03$) and by 9.1% with **BemPPOX** (AUC *BemPPOX group* = 120.1 ± 9.7
 8 $\text{h} \times \text{mg/mL}$), although this latter value was not statistically significant ($p\text{-value} = 0.309$). At $t =$
 9 24 h, AUC ($645.4 \pm 68.0 \text{ h} \times \text{mg/mL}$ in *Control group*) was lowered to 70.9% (AUC *Orlistat group*
 10 = $187.7 \pm 32.5 \text{ h} \times \text{mg/mL}$; $p\text{-value} < 0.01$) and 24.0% (AUC *BemPPOX group* = 490.2 ± 48.0
 11 $\text{h} \times \text{mg/mL}$; $p\text{-value} < 0.05$), in good agreement with the variation of total fatty acid
 12 concentration in lymph.



13
 14 **Fig. 7.** Mean values of the area under the curve (AUC), corresponding to the lymph fatty acid
 15 concentration at times 6 h and 24 h, of the *BemPPOX group* and the *Orlistat group* as compared to the
 16 *Control group* (*i.e.* 100%). Values represent means \pm SEM of at least 7 rats per group, at each time
 17 point. * Mean values are significantly different at a given time point ($p\text{-value} < 0.05$; ANOVA followed
 18 by Fisher's test).

1
2 **Orlistat** is more effective at inhibiting TAG absorption when it is administered in meals
3 rather than after meals [2, 70]. Studies by Isler *et al.* showed that administration of 10 µmol/kg
4 (~5 mg/kg) and 30 µmol/kg (~15 mg/kg) **Orlistat** to mice immediately after the meal resulted
5 in elimination of 20% and 40% of the administered fat, respectively [70]. However, the authors
6 noticed that such doses of **Orlistat** were around 3 times larger compared to those when the
7 inhibitor was dissolved in the lipids of the test meal prior to administration to mice. Taking into
8 account these experiments, both **BemPPOX** and **Orlistat** have been pre-mixed with olive oil
9 and emulsified before being administered directly to the mouth of rats. In the presence of
10 **Orlistat**, the total concentration of absorbed fatty acids (**Figure 6 & Table 3**) from olive oil
11 emulsion was drastically reduced by 53% and 79% as compared to the absorption in control
12 rats after 6 h (*i.e.*, T_{max}) and 24 h, respectively. These data are thus in good agreement with
13 previous *in vivo* experiments [70-72]. When olive oil emulsion was supplemented with
14 **BemPPOX**, the concentration of fatty acids absorbed in the lymph of rats was 31% and 55%
15 lower than the one reached in the *Control group* at the same time points (*i.e.*, 6 h and 24 h,
16 respectively). These *in vivo* data therefore reflect the different inhibitory effects of **Orlistat**
17 (total inhibition of both gastric and duodenal lipolysis) and **BemPPOX** (inhibition of gastric
18 lipolysis only) previously observed *in vitro*.

19 The data obtained *in vivo* in rats indicate that gastric lipolysis by rat lingual lipase is
20 abolished by the action of **BemPPOX**, which impacts the whole gastrointestinal process of lipid
21 digestion and absorption.

22

23 **4. Conclusion**

24 In the present work, a new series of lipophilic compounds based on an oxadiazolone-core
25 were synthesized and their inhibitory effect on various digestive lipases was assessed. Among
26 all tested compounds, **BemPPOX** was found to act in a stoichiometric amount with gastric

1 lipase and also inhibited two pancreatic enzymes, PLRP2 and CEH, but was poorly active on
2 classical pancreatic lipase, the main enzyme involved the intestinal digestion of fats. As a
3 consequence, and contrary to the well-known lipase inhibitor **Orlistat**, **BemPPOX** impaired
4 only gastric lipolysis when test meal were digested *in vitro*. *In vivo*, the administration of
5 **BemPPOX** resulted in a slow-down of the overall lipolysis process and in a 55% decrease in
6 the intestinal absorption of lipids in rats over 24 hours. Taken together, all collected *in vitro* and
7 *in vivo* data not only support the essential role of gastric/lingual lipase in the overall lipolytic
8 process of digestion, but above all they clearly establish that inhibitors specifically designed to
9 block gastric lipolysis are able to monitor the whole gastrointestinal lipolysis and lead to a
10 subsequent reduction of the intestinal absorption of lipids. As a consequence, the expected
11 physiological response of a reduced gastric lipolysis should be an increase of the satiety feelings
12 induced by the “ileal brake” phenomenon [14]. This would radically differ from the action of
13 **Orlistat** that inhibits both gastric and intestinal lipolysis and lowers satiety gut hormone levels
14 (*i.e.*, glucagon-like peptide-1, GLP-1; peptide YY, PYY; and Cholecystokinin, CCK) [13]. In
15 that context, **BemPPOX** should offer the unprecedented opportunity to study the direct effects
16 of the specific inhibition of gastric lipolysis on the postprandial secretion of the satiety
17 hormones and the regulation of food intake, and may provide a new approach in the struggle
18 against obesity.

19

20

1 **5. Experimental Section**

2 *5.1. Chemistry*

3 *5.1.1. General methods of Synthesis*

4 Commercially available starting materials were purchased from Sigma-Aldrich (St Quentin
5 Fallavier, France) and used without further purification. All reactions were carried out under
6 strictly anhydrous conditions; and all solvents were purified according to usual methods [73].

7 Analytical thin-layer chromatography (TLC) was carried out on Merck silica gel F₂₅₄ (60 Å,
8 40–63 µm, 230–400 mesh) pre-coated aluminium sheets, and the following detection methods
9 were used: UV lamp (254 nm) and PMA: dipped into a solution containing 5%
10 phosphomolybdic acid in absolute ethanol, and heated on a hot plate. Flash chromatography
11 separations were performed using Merck silica gel 60 (230-400 mesh) according to Still *et al.*

12 [74]. ¹H and ¹³C NMR spectra were recorded on BRUKER Avance 200 spectrometer operating
13 at 200 MHz for ¹H and 50 MHz for ¹³C. Chemical shifts are reported in ppm on the δ scale from
14 an internal standard of solvent (CDCl₃, δ = 7.27 ppm for ¹H NMR and 77.23 ppm in ¹³C NMR).

15 Coupling constants (*J*) are reported in hertz. ¹H spectral splitting patterns are designated as s,
16 singlet; d, doublet; t, triplet; q, quartet; quint, quintet; sext, sextet; sept, septet; m, multiplet. ¹³C
17 spectral splitting patterns are designated as s, singlet (quaternary elements); d, doublet (CH); t,
18 triplet (CH₂); q, quartet (CH₃). Accurate mass measurements (HRMS) were performed with a
19 QStar Elite mass spectrometer equipped with an electrospray ionization source (ESI), operated
20 in the positive mode. In this hybrid instrument, ions were measured using an orthogonal
21 acceleration time-of-flight (oa-TOF) mass analyzer. Infrared spectra were recorded on a
22 Thermo-Nicolet IR 200 spectrophotometer. Melting points were measured using a Büchi B–
23 545.

24 High-performance liquid chromatography analyses were used to confirm the purity of all
25 compounds (≥ 97%), and were performed on a Waters 600 equipment, at a flow rate of 1
26 mL/min, with a UV photodiode-array detector (Waters 2998 PAD detector), and using a C18

1 reversed phase column Waters XBridge C18 (4.6 × 100 mm, 3.5 µm particle size). The elution
2 was performed with a mixture of acetonitrile and water under acidic conditions (*i.e.*, 0.01%
3 trifluoroacetic acid).

4

5 *5.1.2. Preparation of (3-phenoxyphenyl)hydrazine hydrochloride (1)*

6 As previously described [23], (3-phenoxyphenyl)hydrazine hydrochloride **1** was obtained from
7 commercial 3-phenoxyaniline (Sigma-Aldrich) as a pink amorphous solid (6.11 g, 68.4%).
8 Analytical data for **1**: mp 186–188 °C; IR (neat) ν 3174–2847 (N-H); For NMR analysis, the
9 free hydrazine was released by action of 50% NaOH solution. R_f (AcOEt/hexane 1:9, v/v) 0.43.
10 ^1H NMR (200 MHz, CDCl_3) δ (ppm) 7.38 – 7.29 (m, 2H), 7.17 (app t, J = 7.4 Hz, 1H), 7.09 –
11 6.98 (m, 3H), 6.58 – 6.52 (m, 1H), 6.51 – 6.48 (m, 1H), 6.44 (m, 1H), 5.34 – 5.07 (m, 1H), 3.63
12 – 3.45 (m, 2H). ^{13}C NMR (50 MHz, CDCl_3) δ (ppm) 158.4 (s), 157.1 (s), 152.9 (s), 130.1 (d),
13 129.6 (2 × d), 123.1 (d), 118.9 (2 × d), 109.4 (d), 107.0 (d), 102.5 (d).

14

15 *5.1.3. General procedure for the one step preparation of 5-alkoxy-3-(3-phenoxyphenyl)-1,3,4-*
16 *oxadiazol-2(3H)-one compounds RmPPOX (3a-j) from 3-phenoxy-phenylhydrazine (1).*

17 *5.1.3.1. 5-(2-(benzyloxy)ethoxy)-3-(3-phenoxyphenyl)-1,3,4-oxadiazol-2(3H)-one (3a) =*
18 *BemPPOX).*

19 (3-phenoxyphenyl)hydrazine hydrochloride **1** (10 g, 42.2 mmol, 1 equiv.) was dissolved in dry
20 pyridine (100 mL). The solution was cooled to 0 °C with an ice bath over a 30-min period.
21 2-benzyloxyethyl chloroformate **2a** (10 g, 8.4 mL, 46.4 mmol, 1.1 equiv.) was then added
22 dropwise over a period of 30 min at 0–5 °C and allowed to stir for 24 h at room temperature.
23 The reaction mixture was diluted by addition of methylene chloride (800 mL) and dry pyridine
24 (100 mL) and stirred for additional 30 min at –10 °C using an ice-salt bath. A solution of
25 diphosgene (9.18 g, 5.6 mL, 46.4 mmol, 1.1 equiv.) in methylene chloride (100 mL) was added
26 dropwise using a drooping funnel over a period of 30 min while maintaining –10 °C with an

1 ice-salt bath. After the addition is complete the reaction mixture was brought to room
2 temperature and stirred 24h. The reaction mixture was diluted with water (500 mL) and
3 extracted with diethyl ether (3×500 mL). The combined organic layers were washed with
4 water (500 mL) and brine (2×200 mL), dried over Na_2SO_4 , and filtered. Purification by column
5 chromatography using Et_2O /petroleum ether (30:70, *v/v*) as eluent gave the title compound **3a**
6 as a light beige powder (6.57 g, 38.5%).

7 For *in vivo* experiments purpose, compound **3a** was further recrystallized with pentane/ AcOEt
8 to give a white solid (4.85 g, 28.4%). Analytical data for **3a**: mp: 59–61 °C. R_f (Et_2O /petroleum
9 ether 30:70, *v/v*) 0.37. IR (neat) ν 1797 (C=O), 1657 (C=N) cm^{-1} . HRMS (ESI) *m/z* [M+H]⁺
10 calcd. for $\text{C}_{23}\text{H}_{21}\text{N}_2\text{O}_5$: 405.1445 Da; found: 405.1446 Da. ^1H NMR δ 7.57 (ddd, *J* = 8.2, 2.1,
11 0.9 Hz, 1H), 7.48 (t, *J* = 2.2 Hz, 1H), 7.42 – 7.27 (m, 8H), 7.17 – 7.09 (m, 1H), 7.07 – 7.00 (m,
12 2H), 6.83 (ddd, *J* = 8.2, 2.4, 0.9 Hz, 1H), 4.61 (s, *J* = 8.0 Hz, 2H), 4.57 – 4.51 (m, 2H), 3.92 –
13 3.74 (m, 2H). ^{13}C NMR δ 157.86 (s), 156.70 (s), 155.11 (s), 147.90 (s), 137.49 (s), 137.46 (s),
14 130.18 (s), 129.79 (2 × d), 128.42 (2 × d), 127.82 (d), 127.64 (2 × d), 123.59 (d), 118.96 (2 × d),
15 115.40 (d), 112.41 (d), 108.72 (d), 73.21 (t), 70.57 (t), 66.90 (t).

16 ^1H and ^{13}C NMR spectra as well as HPLC profile and HRMS spectrum of **BemPPOX** are shown
17 on **Supplementary Data Figs S4-S7**.

18

19 **5.1.3.2. 5-ethoxy-3-(3-phenoxyphenyl)-1,3,4-oxadiazol-2(3*H*)-one (3b = **EmPPOX**).**

20 Prepared using Ethyl chloroformate **2b** applying similar method as described above for **3a**.
21 Yellow crystals (283 mg, 44.8%). Analytical data for **3b**: mp: 50–51 °C. R_f (Et_2O /petroleum
22 ether 20:80, *v/v*) 0.50. IR (neat) ν 1791 (C=O), 1656 (C=N) cm^{-1} . HRMS (ESI) *m/z* [M+H]⁺
23 calcd. for $\text{C}_{16}\text{H}_{15}\text{N}_2\text{O}_4$: 299.1026 Da; found: 299.1031 Da. ^1H NMR δ 7.58 (dd, *J* = 8.2, 1.2 Hz,
24 1H), 7.49 (t, *J* = 2.1 Hz, 1H), 7.35 (t, *J* = 7.9 Hz, 3H), 7.13 (t, *J* = 7.4 Hz, 1H), 7.03 (d, *J* = 7.7
25 Hz, 2H), 6.82 (dd, *J* = 8.2, 1.7 Hz, 1H), 4.45 (q, *J* = 7.1 Hz, 2H), 1.48 (t, *J* = 7.1 Hz, 3H). ^{13}C

1 NMR δ 157.53 (s), 156.42 (s), 154.75 (s), 147.69 (s), 137.22 (s), 129.84 (d), 129.45 (2 × d)
2 123.24 (d), 118.61 (2 × d), 115.02 (d), 112.08 (d), 108.42 (d), 67.47 (t), 13.66 (q).

3

4 **5.1.3.3. 5-butyloxy-3-(3-phenoxyphenyl)-1,3,4-oxadiazol-2(3H)-one (3c = *BmPPOX*)**

5 Prepared using Butyl chloroformate **2c** applying similar method as described above for **3a**. Pale
6 yellow sticky liquid (295 mg, 43.0%). Analytical data for **3c**: R_f (AcOEt/petroleum ether 5:95,
7 v/v) 0.30. IR (neat) ν 1796 (C=O), 1658 (C=N) cm⁻¹. HRMS (ESI) *m/z* [M+H]⁺ calcd. for
8 C₁₈H₁₉N₂O₄: 327.1339 Da; found: 327.1338 Da. ¹H NMR δ 7.59 (ddd, *J* = 8.2, 2.1, 0.9 Hz, 1H),
9 7.50 (t, *J* = 2.2 Hz, 1H), 7.41 – 7.30 (m, 3H), 7.17 – 7.08 (m, 1H), 7.07 – 6.99 (m, 2H), 6.83
10 (ddd, *J* = 8.2, 2.4, 0.9 Hz, 1H), 4.38 (t, *J* = 6.5 Hz, 2H), 1.89 – 1.74 (m, 2H), 1.58 – 1.40 (m,
11 2H), 0.99 (t, *J* = 7.3 Hz, 3H). ¹³C NMR δ 157.00 (s), 155.89 (s), 154.40 (s), 147.20 (s), 136.67
12 (s), 129.30 (d), 128.90 (2 × d), 122.68 (d), 118.07 (2 × d), 114.54 (d), 111.60 (d), 107.97 (d),
13 70.65 (t), 29.41 (t), 17.80 (t), 12.61 (q).

14

15 **5.1.3.4. 5-isobutoxy-3-(3-phenoxyphenyl)-1,3,4-oxadiazol-2(3H)-one (3d = *iBmPPOX*)**

16 Prepared using Isobutyl chloroformate **2d** applying similar method as described above for **3a**.
17 White amorphous powder (272 mg, 45.0%). Analytical data for **3d**: mp: 38-40 °C. R_f
18 (Et₂O/petroleum ether 5:95, v/v) 0.28. IR (neat) ν 1797 (C=O), 1660 (C=N) cm⁻¹. HRMS (ESI)
19 *m/z* [M+H]⁺ calcd. for C₁₈H₁₉N₂O₄: 327.1339 Da; found: 327.1339 Da. ¹H NMR δ: 7.58 (ddd,
20 *J* = 8.2 Hz, *J* = 2.3 Hz, *J* = 0.8 Hz, 1H), 7.49 (t, *J* = 2.2 Hz, 1H), 7.35 (t, *J* = 7.7 Hz, 3H), 7.12
21 (t, *J* = 7.4 Hz, 1H), 7.03 (d, *J* = 8.8 Hz, 2H), 6.82 (ddd, *J* = 8.2 Hz, *J* = 2.3 Hz, *J* = 0.8 Hz 1H),
22 4.15 (d, *J* = 6.6 Hz, 2H), 2.10 (d, *J* = 21.1 Hz, 1H), 1.04 (s, 3H), 1.01 (s, 3H). ¹³C NMR δ:
23 158.01 (s), 156.95 (s), 155.53 (s), 148.26 (s), 137.69 (s), 130.36 (d), 129.94 (2 × d), 123.70 (d),
24 119.08 (2 × d), 115.65 (d), 112.70 (d), 109.11 (d), 77.59 (t), 27.84 (s), 18.78 (2 × q).

25

26 **5.1.3.5. 5-hexyloxy-3-(3-phenoxyphenyl)-1,3,4-oxadiazol-2(3H)-one (3e = *HmPPOX*)**

1 Prepared using Hexyl chloroformate **2e** applying similar method as described above for **3a**.
2 White crystalline solid (216 mg, 44.0%). Analytical data for **3e**: mp 48-50 °C. R_f
3 (Et₂O/petroleum ether 5:95, v/v) 0.20. IR (neat) ν 1796 (C=O), 1671 (C=N) cm⁻¹. HRMS (ESI)
4 m/z [M+H]⁺ calcd. for C₂₀H₂₃N₂O₄: 355.1652 Da; found: 355.1652 Da. ¹H NMR δ 7.58 (ddd,
5 J = 8.2, 2.1, 0.9 Hz, 1H), 7.49 (t, J = 2.2 Hz, 1H), 7.40 – 7.30 (m, 3H), 7.12 (ddd, J = 6.7, 4.0,
6 1.1 Hz, 1H), 7.07 – 6.99 (m, 2H), 6.82 (ddd, J = 8.2, 2.4, 0.9 Hz, 1H), 4.37 (t, J = 6.6 Hz, 2H),
7 1.91 – 1.74 (m, 2H), 1.46 – 1.26 (m, 6H), 0.91 (s, J = 6.4 Hz, 3H). ¹³C NMR δ 157.97 (s),
8 156.88 (s), 155.38 (s), 148.18 (s), 137.65 (s), 130.29(d), 129.88 (2 × d), 123.66 (d), 119.05
9 (2 × d), 115.53 (d), 112.58 (d), 108.96 (d), 71.94 (t), 31.30 (t), 28.38 (t), 25.20 (t), 22.54 (t),
10 14.02 (q).

11

12 **5.1.3.6. 5-octyloxy-3-(3-phenoxyphenyl)-1,3,4-oxadiazol-2(3H)-one (3f = OmPPOX)**
13 Prepared using Octyl chloroformate **2f** applying similar method as described above for **3a**. Light
14 beige powder (433 mg, 47.0%). Analytical data for **3f**: mp 49-50 °C. R_f (AcOEt/petroleum ether
15 20:80, v/v) 0.85. IR (neat) ν 1790 (C=O), 1660 (C=N) cm⁻¹. HRMS (ESI) m/z [M+H]⁺ calcd.
16 for C₂₂H₂₇N₂O₄: 383.1965 Da; found: 383.1969 Da. ¹H NMR δ 7.58 (ddd, J = 8.2, 2.1, 0.9 Hz,
17 1H), 7.49 (t, J = 2.2 Hz, 1H), 7.35 (t, J = 7.6 Hz, 3H), 7.18 – 7.08 (m, 1H), 7.03 (d, J = 7.5 Hz,
18 2H), 6.82 (ddd, J = 8.2, 2.4, 0.9 Hz, 1H), 4.37 (t, J = 6.6 Hz, 2H), 1.92 – 1.68 (m, 2H), 1.24 (d,
19 J = 19.9 Hz, 10H), 0.99 – 0.77 (m, 3H). ¹³C NMR δ 158.03 (s), 156.94 (s), 155.45 (s), 148.28
20 (s), 137.69 (s), 130.36 (d), 129.95 (2 × d), 123.72 (d), 119.11 (2 × d), 115.64 (d), 112.69 (d),
21 109.08 (d), 72.00 (t), 31.85 (t), 29.21 (t), 29.16 (t), 28.48 (t), 25.59 (t), 22.74 (t), 14.19 (q).

22

23 **5.1.3.7. 5-decyloxy-3-(3-phenoxyphenyl)-1,3,4-oxadiazol-2(3H)-one (3g = DmPPOX)**
24 Prepared using Decyl chloroformate **2g** applying similar method as described above for **3a**.
25 Pale yellow powder (427 mg, 49.3%). Analytical data for **3g**: mp 56-57 °C. R_f (Et₂O/petroleum
26 ether 5:95, v/v) 0.40. IR (neat) ν 1791 (C=O), 1661 (C=N) cm⁻¹. HRMS (ESI) m/z [M+H]⁺

1 calcd. for C₂₄H₃₁N₂O₄: 411.2276 Da; found: 411.2278 Da. ¹H NMR δ 7.58 (ddd, *J* = 8.1, 2.0,
2 0.9 Hz, 1H), 7.49 (t, *J* = 2.1 Hz, 1H), 7.40 – 7.30 (m, 3H), 7.17 – 6.99 (m, 3H), 6.82 (ddd, *J* =
3 8.2, 2.4, 0.9 Hz, 1H), 4.37 (t, *J* = 6.6 Hz, 2H), 1.80 (dd, *J* = 13.8, 6.9 Hz, 2H), 1.47 – 1.20 (m,
4 17H). ¹³C NMR δ 157.84 (s), 156.75 (s), 155.27 (s), 154.53 (s), 137.51 (s), 130.18 (d), 129.77
5 (2 × d), 129.53 (d), 123.53 (d), 118.92 (2 × d), 115.46 (d), 112.51 (d), 108.91 (d), 71.82 (t),
6 31.81 (t), 29.78 (t), 29.38 (t) 28.82 (t), 28.30 (t), 25.41 (t), 22.61 (t), 14.05 (q).

7

8 **5.1.3.8. 5-dodecyloxy-3-(3-phenoxyphenyl)-1,3,4-oxadiazol-2(3H)-one (3h = DomPPOX)**

9 Prepared using Dodecyl chloroformate **2h** applying similar method as described above for **3a**.
10 White powder (220 mg, 43.4%). Analytical data for **3h**: mp 65–66 °C. *R*_f (Et₂O/petroleum ether
11 5:95, v/v) 0.37. IR (neat) *v* 1791 (C=O), 1660 (C=N) cm⁻¹. HRMS (ESI) *m/z* [M+H]⁺ calcd. for
12 C₂₆H₃₅N₂O₄: 439.2591 Da; found: 439.2595 Da. ¹H NMR δ 7.58 (ddd, *J* = 8.2, 2.1, 0.9 Hz, 1H),
13 7.49 (t, *J* = 2.2 Hz, 1H), 7.40 – 7.30 (m, 3H), 7.17 – 7.08 (m, 1H), 7.07 – 6.99 (m, 2H), 6.82
14 (ddd, *J* = 8.2, 2.4, 0.9 Hz, 1H), 4.37 (t, *J* = 6.6 Hz, 2H), 1.90 – 1.75 (m, 2H), 1.41 – 1.23 (m,
15 18H), 0.88 (t, *J* = 6.1 Hz, 3H). ¹³C NMR δ 158.06 (s), 156.97 (s), 155.48 (s), 137.73 (s), 130.35
16 (d), 129.95 (2 × d), 123.72 (d), 119.12 (2 × d), 115.64 (d), 112.70 (d), 109.09 (d), 72.01 (t),
17 65.97 (t), 32.04 (t), 29.74 (2 × t), 29.65 (t), 29.56 (t), 29.46 (t), 29.21 (t), 28.50 (t), 25.60 (t), 22.81
18 (t), 15.39 (t), 14.22 (q).

19

20 **5.1.3.10. 5-(2-ethylhexyloxy)-3-(3-phenoxyphenyl)-1,3,4-oxadiazol-2(3H)-one (3i =**
21 **EhmPPOX)**

22 Prepared using 2-Ethylhexyl chloroformate **2i** applying similar method as described above for
23 **3a**. Yellow oil (360 mg, 45.1%). Analytical data for **3i**: *R*_f (AcOEt/petroleum ether 5:95, v/v)
24 0.60. IR (neat) *v* 1798 (C=O), 1657 (C=N) cm⁻¹. HRMS (ESI) *m/z* [M+H]⁺ calcd. for
25 C₂₂H₂₇N₂O₄: 383.1965 Da; found: 383.1967 Da. ¹H NMR δ 7.59 (ddd, *J* = 8.2, 2.1, 0.9 Hz, 1H),
26 7.50 (t, *J* = 2.2 Hz, 1H), 7.41 – 7.29 (m, 3H), 7.17 – 7.08 (m, 1H), 7.07 – 6.99 (m, 2H), 6.82

1 (ddd, $J = 8.2, 2.4, 0.9$ Hz, 1H), 4.28 (d, $J = 5.7$ Hz, 2H), 1.86 – 1.68 (m, 1H), 1.49 – 1.26 (m,
2 8H), 0.98 – 0.87 (m, 6H). ^{13}C NMR δ 157.99(s), 156.90(s), 155.56(s), 148.17 (s), 137.88(s),
3 130.28(d), 129.88 (2 \times d), 123.65(d), 119.05 (2 \times d), 115.53(d), 112.57(d), 108.96 (d), 74.14
4 (d), 38.89 (t), 30.18(d), 28.90(t), 23.49(t) 22.95 (t), 14.06(q), 10.99(q).

5

6 5.1.3.10. 5-(2-methoxyethoxy)-3-(3-phenoxyphenyl)-1,3,4-oxadiazol-2(3H)-one (3j) =
7 **MemPPOX**)

8 Prepared from 2-methoxyethyl chloroformate **2j** applying similar method as described above
9 for **3a**. Light beige powder (416 mg, 43.5%). Analytical data for **3j**: mp 67-69 °C. R_f
10 (AcOEt/petroleum ether 10:90, v/v) 0.20. IR (neat) ν 1786 (C=O), 1660 (C=N) cm⁻¹. HRMS
11 (ESI) m/z [M+H]⁺ calcd. for C₁₇H₁₇N₂O₅: 329.1132 Da; found: 329.1131 Da. ^1H NMR δ 7.56
12 (ddd, $J = 8.2, 2.1, 1.0$ Hz, 1H), 7.47 (t, $J = 2.1$ Hz, 1H), 7.40 – 7.28 (m, 3H), 7.16 – 7.06 (m,
13 1H), 7.05 – 6.97 (m, 2H), 6.81 (ddd, $J = 8.2, 2.4, 0.9$ Hz, 1H), 4.54 – 4.43 (m, 2H), 3.77 – 3.68
14 (m, 2H), 3.41 (s, 3H). ^{13}C NMR δ 157.84 (s), 156.59 (s), 155.20 (s), 147.85 (s), 137.43 (s),
15 130.12 (d), 129.72 (2 \times d), 123.54 (d), 118.91 (2 \times d), 115.30 (d), 112.31 (d), 108.60 (d), 70.40
16 (t), 69.39 (t), 58.89 (q).

17

18 5.2. *In vitro inhibition tests*

19 5.2.1. *Reagents*

20 All reactive and reagents, including **Orlistat**, were purchased from Sigma-Aldrich-Fluka
21 Chimie (St-Quentin-Fallavier, France). All organic solvents were purchased from Carlo Erba
22 Reactifs-SDS (Val de Reuil, France) and were of HPLC grade.

23

24 5.2.2. *Enzymes*.

25 All lipases were produced and purified to homogeneity. Recombinant guinea pig pancreatic
26 lipase-related protein 2 (GPLRP2) was expressed in *Aspergillus orizae* and purified according

1 to [32]. Recombinant dog gastric lipase (DGL) was produced in transgenic maize by Meristem
2 Therapeutics (Clermont-Ferrand, France) [75] and purified as described previously [30]. Native
3 human pancreatic carboxylic ester hydrolase (*hCEH*) was purified to homogeneity from
4 pancreatic juice according to the method previously described [76]. Porcine pancreatic extracts
5 (PPE), also named pancreatin (P7545; 8× USP grade) which contain around 1.0 wt% of porcine
6 pancreatic lipase (PPL) were purchased from Sigma-Aldrich-Fluka Chimie (St-Quentin-
7 Fallavier, France).

8 Human pancreatic juice (HPJ) was collected from healthy volunteers with no digestive
9 pathologies at the Sainte-Marguerite Hospital (Marseille), under the supervision of Professor
10 René Laugier by performing retrograde endoscopic catheterization on the main pancreatic duct
11 [77]. The pancreatic juice samples were immediately mixed with a solution of protease
12 inhibitors, phenylmethane sulfonyl fluoride and benzamidine, each at a final concentration of 2
13 mM. The mixture was immediately lyophilized and the resulting powder was stored at -20 °C
14 before use.

15 A protein extract containing rat lingual lipase (RLL) was obtained from serous glands of rat
16 tongues as described in [78]. The homogenate of the lingual serous glands in cold 150 mM
17 NaCl was centrifuged at 100,000 × *g* for 60 min. The supernatant, containing the lipase activity,
18 was precipitated with 30-60% saturated ammonium sulfate. The protein precipitate was
19 solubilized in 4.5 mM citric acid, 11 mM Na₂HPO₄ buffer at pH 5.4, and an additional protein
20 precipitation was performed by mixing this solution with 2 vol. of cold acetone at -20 °C. After
21 centrifugation, the recovered proteins were solubilized in buffered solution at pH 5.4. The
22 mixture was centrifuged at 12,000 × *g* at -10 °C for 20 min and the clear supernatant was
23 separated and lyophilized. The resulting powder containing RLL (0.24% w/w) was further
24 stored at -20 °C before use.

25

26 *5.2.3. Lipase activity measurements using the pH-stat technique.*

1 Enzymatic activity was assayed at 37°C by measuring the amount of free fatty acid (FFA)
2 released from a mechanically stirred tributyrin (TC4) emulsion, using 0.1 N NaOH with a pH-
3 stat (Metrohm 718 STAT Titrino, Switzerland) adjusted to a fixed end point value as previously
4 described [23, 36]. The triacylglycerol emulsions were formed by mixing 0.5 mL TC4 with
5 14.5 mL buffer solution. The activity of pancreatic lipase contained in human pancreatic juice
6 or PPE was determined at pH 8.0 using the standard assay solution: 0.3 mM Tris-HCl, 150 mM
7 NaCl, 2 mM CaCl₂, and 4 mM sodium taurodeoxycholate (NaTDC) [79]. The assay solution
8 for GPLRP2 was 1 mM Tris-HCl (pH 8.0), 150 mM NaCl, 5 mM CaCl₂ and 2 mM NaTDC
9 [32]. In the case of DGL and RLL, the assay solution was 150 mM NaCl, 2 mM NaTDC, 1.5
10 µM BSA at pH 5.5 [80]. The assay solution used with *hCEH* was 1 mM Tris-HCl (pH 8.0), 100
11 mM NaCl, 5 mM CaCl₂, containing 1 mM NaTDC [81]. All experiments were performed at
12 least in triplicate. Activities were expressed as international units: 1 U = 1 µmol FFA released
13 per minute. The specific activities of GPLRP2, DGL and *hCEH*, expressed in U per mg of pure
14 enzyme, were found to be 2,270 ± 33, 340 ± 21 and 318 ± 7 U/mg, respectively. The lipase
15 activity of lyophilized proteins from rat tongue extract was found to be 2.4 ± 0.04 U per mg of
16 lyophilized powder, which corresponds to around 0.24 wt% of RLL. The lipase activities of
17 HPJ and PPE were found to be 218 ± 7 and 254 ± 13 U per mg of lyophilized powder,
18 respectively, which corresponds to around 2.7 wt% of HPL and 1.0 wt% of PPL.

19
20 *5.2.4. Inhibition assays.*

21 The lipase-inhibitor pre-incubation method was used to test in aqueous medium and in the
22 absence of substrate, the possible direct reactions between lipases and inhibitors as previously
23 described [23]. Stock solutions (4 mg/mL) of each inhibitor were prepared in dimethyl sulfoxide
24 (DMSO). The following lipases stock solutions were used: 2 mg/mL HPJ (*i.e.*, 54 µg/mL HPL)
25 or 3.2 mg/mL PPE (*i.e.*, 32 µg/mL PPL) in 10 mM MES (pH 7.0), 150 mM NaCl; 0.5 mg/mL
26 GPLRP2 in 20 mM Tris (pH 8.0), 1 mM Benzamidine; 0.1 mg/mL DGL or 10 mg/mL rat

1 tongue extract (*i.e.*, 24 µg/mL RLL) in 10 mM MES (pH 6.0), 150 mM NaCl; and 1 mg/mL
2 *hCEH* in 10 mM MES (pH 6.5), 150 mM NaCl. These enzyme solutions were used for enzyme-
3 inhibitor pre-incubation for 30 min at 25°C at various inhibitor molar excess (x_I) related to 1
4 mole of lipase.

5 Lipase incubations with inhibitors were performed in the presence of 4 mM NaTDC in the case
6 of HPJ, PPE, DGL and RLL, and 2 mM NaTDC with GPLRP2 inhibition assays [82]. The
7 presence of bile salts (NaTDC) favors the opening of the molecular lid controlling the access
8 to the active site of gastric and pancreatic lipases [83], as well as inhibition kinetics [84]. During
9 the inhibition experiments performed with various inhibitor to lipase molar excess, samples of
10 the incubation medium were collected for measuring residual lipase activity, that was further
11 used to determine the molar excess of the inhibitor which reduced the enzyme activity to 50%
12 of its initial value (x_{I50}) [23]. In addition, the enzymes were also pre-incubated at 25 °C with
13 selected inhibitor at a fixed molar excess ($x_I = 2$ with GPLRP2; $x_I = 20$ with DGL and RLL;
14 and $x_I = 4$ with *hCEH*) for 1 hour; and the residual enzyme activity was measured at various
15 time intervals in order to determine the half-inactivation time ($t_{1/2}$) corresponding to 50%
16 residual enzyme activity [85]. In each case, control experiments were performed in the absence
17 of inhibitor but with the same volume of DMSO. It is worth noting that DMSO at a final volume
18 concentration of less than 10% has no effect on the enzyme activity.

19
20 *5.2.5. Molecular docking.*

21 *In silico* molecular docking of lipase inhibitors present in the active site of DGL was performed
22 with the Autodock Vina program [86] as previously described [23]. The PyMOL Molecular
23 Graphics System (version 1.4, Schrödinger, LLC) was used as working environment with an
24 in-house version of the AutoDock/Vina PyMOL plugin [87]. The X-ray crystallographic
25 structures of DGL (PDB entry code: 1K8Q; 2.70 Å resolution [30]), GPLRP2-HPL chimera
26 (PDB entry code: 1GPL; 2.01 Å resolution [33]) and *hCEH* (PDB entry code: 1F6W; 2.30 Å

1 resolution [50]) available at the Protein Data Bank were used as receptors. Docking runs were
2 performed after replacing the catalytic serine by a glycine residue to enable the ligand to adopt
3 a suitable position corresponding to the pre-bound intermediate before the nucleophilic attack
4 in the lipase active site. The box size used for the various receptors was chosen to fit the whole
5 active site cleft and to allow non constructive binding positions. A model structure file was
6 generated for each inhibitor molecule, and its geometry was refined using the Avogadro open-
7 source program (version 1.1.1. <http://avogadro.openmolecules.net/>).

8

9 *5.3 In vitro simulation of the gastrointestinal lipolysis*

10 *In vitro* lipolysis experiments were performed using a two-step static digestion model with a
11 gastric phase followed by a duodenal phase [25]. Experimental conditions were adapted from
12 *in vivo* data recorded at 50% gastric emptying of test meals, both in the stomach and in the
13 duodenum; and enzymatic solutions were prepared according to *in vivo* secretions of human
14 digestive lipases during a meal [2, 15, 52].

15

16 *5.3.1 Test meals*

17 *Ensure Plus*® (Therapeutic Nutrition Shake Vanilla bottle; Abbott Nutrition) was used as a
18 complete liquid test meal containing lipids, proteins and carbohydrates. Extraction of the total
19 lipids followed by TAG quantification by TLC-FID [60] showed that a standard 237-mL bottle
20 contains around 10.9 g of TAGs (12.3 mmol) originating from corn oil, rapeseed oil and
21 soybean oil. For the *in vitro* simulation of the gastrointestinal lipolysis, the liquid test meal
22 consisted of 15 mL (9.7 mL of Ensure Plus and 5.3 mL of tap water) corresponding to 450 mg
23 (0.51 mmol) of TAGs.

24 A mixed solid-liquid test meal was also prepared and is referred to here as the solid test meal
25 [2, 25]. This solid test meal was prepared by mixing 80 g string beans, 90 g grilled beef meat,
26 70 g French fries, 10 g butter, 20 g sunflower oil and tap water, making a total volume of 700

1 mL. All these ingredients were purchased at local grocery stores (Marseille, France). The butter
2 and sunflower oil were used for cooking the beans and the fries, respectively. For the *in vitro*
3 assays, the meal was first prepared without water: after all the ingredients had been cooked
4 separately, they were mixed and passed through a mincer with a 2-mm grid aperture in order to
5 obtain a homogeneous paste. The paste was then divided in 5.8 g aliquots, which were stored
6 at -20 °C before use. For each *in vitro* assay, 5.8 g of this solid formula were mixed with 9.2
7 mL tap water in order to reconstitute 15 mL equivalent of test meal. Water was added to the
8 paste just before the beginning of experiments so that the meal components do not separate for
9 a better reproducibility of the procedure [25]. The TAGs concentration present into the meal
10 was estimated to be 87.3 mg/g by extracting the total lipids with chloroform-methanol and
11 quantifying TAGs using TLC-FID [60]. Each *in vitro* assay was thus performed with 15 mL
12 equivalent of test meal, containing 506 mg TAGs.

13

14 *5.3.2 Preparation of inhibitor and digestive enzymes solutions*

15 *5.3.2.1 Inhibitor solutions*

16 Stock solutions of **Orlistat** (4.9 mg/mL) and **BemPPOX** (4.1 mg/mL) were prepared in DMSO.
17 The meal volume-to-drug dose ratio was kept identical to the ratio used for *in vivo* experiments
18 (500-mL meal with 120 mg of Orlistat) [2]. Before the gastric lipase solution was added, 734
19 µL of either **Orlistat** (*i.e.*, 3.6 mg or 7.262 µmol) solution or **BemPPOX** (*i.e.*, 2.94 mg or 7.262
20 µmol) solution were premixed with the meal. Control experiments were performed without
21 inhibitor but with the same volume of DMSO.

22 *5.3.2.2 Solution of DGL) for simulating gastric juice*

23 To mimic human gastric juice [15], a 100 µg/mL DGL solution was prepared in 10 mM MES,
24 150 mM NaCl buffer at pH 6.0), this pH value allowing an optimum stability of DGL before
25 the digestion assays.

1 5.3.2.3 *Mixture of porcine pancreatic extracts and bovine bile for simulating pancreatic and*
2 *biliary secretions*

3 Bile was reconstituted by dissolving 71.4 mg of bovine bile powder (Sigma ref. 3883) in 1.6
4 mL of 10 mM Tris and 150 mM NaCl, (pH 6.0) for a total bile salt concentration of around 63
5 mM. A solution of pancreatic enzymes and bile was obtained by mixing 637.5 mg of PPE (*i.e.*,
6 6.375 mg PPL) with 1.6 mL bovine bile solution and 150 mM NaCl solution to obtain a total
7 volume of 10.5 mL. The bile salt and PPL concentrations in this solution were 9.6 mM and 607
8 µg/mL, respectively.

9

10 5.3.3 *In vitro Gastrointestinal Lipolysis Experiments*

11 Each experiment was performed in a 50-mL thermostated (37 °C) vessel equipped with a pH
12 electrode and a 1-cm magnetic bar rotating at a speed of 1,000 rpm, as described previously [2,
13 25]. At time 0, the meal (15 mL), with or without inhibitor, was mixed with 3-mL gastric lipase
14 solution freshly prepared to obtain a final concentration of 17 µg/mL of DGL, and the pH value
15 was adjusted to 5.5 (gastric step of lipolysis). One-milliliter samples were collected at $t = 1$, 15
16 and 29 min for analysis. The pancreatic juice and bile mixture (10.5 mL) freshly prepared was
17 added at $t = 30$ min and the pH value was adjusted to 6.25 (duodenal step of lipolysis). The total
18 volume at $t = 30$ min was 25.5 mL, therefore corresponding to a 1.7-fold dilution of the gastric
19 phase to simulate the dilution of gastric contents in the upper small intestine. The final PPL and
20 bile salt concentrations in the incubation vessel were then 250 µg/mL and 4.0 mM, respectively.
21 One-milliliter samples were collected at $t = 35$, 40, 45, 60, and 90 min. These 1-mL samples
22 were used immediately after being collected to measure residual lipase activities (pH-stat
23 technique) and to extract the lipids.

24

25 5.3.4 *Lipid Extraction*

1 Lipid extraction was performed immediately after sampling using the procedure of Folch et al.
2 [88] as previously described [25, 60]. One milliliter of the reaction mixture was mixed
3 vigorously with 200 µL 0.1 N HCl and 5 mL chloroform/methanol (2:1 v/v) in a 15-mL glass
4 tube with a screw cap. After phase separation, the lower organic phase was collected using a
5 Pasteur pipette and transferred to a 15-mL test tube, in which it was dried over anhydrous
6 MgSO₄. The clear dried organic lipid extract (nearly 3.50 mL) was transferred to a 5-mL vial
7 with a screw cap, and the vial was kept at -20 °C until the lipid analysis was performed.

8

9 *5.3.5 TLC-FID Analysis of Lipolysis Products*

10 Triacylglycerols (TAG), diacylglycerols (DAG), monoacylglycerols (MAG) and free fatty
11 acids (FFA) were separated on silica-coated quartz rods (SIII Chromarods) and quantified by
12 TLC–FID using a MK-5 Iatroskan apparatus (Iatron, Japan) as previously reported in [25, 60].
13 Briefly, using a 2-µL Hamilton syringe, 1.0 µL of each lipid extract was spotted onto the
14 chromarod and the elution was performed with n-heptane/diethyl ether/formic acid (55/45/1
15 v/v/v) as the migration solvent. After 25 min, the chromarod holder (10 chromarods) was
16 removed from the TLC tank and the chromarods were dried at 150 °C for 15 min. The
17 chromarod holder was then placed in the Iatroskan MK5 apparatus and each chromarod was
18 scanned with the FID to detect and quantify the compounds separated on silica rods. Known
19 amounts (0.4 to 6 µg) of standard compounds (triolein, diolein, monoolein and oleic acid) were
20 used to calibrate the mass detection by FID and also validate the method [60]. For each class of
21 compound analyzed, a calibration curve (peak area *vs.* mass) was established and used to
22 quantify the lipid masses in the various samples. The mass detection data were further converted
23 into moles using the molar masses estimated from the fatty acid composition of the test meals:
24 883 g/mole for TAG, 619 g/mole for DAG, 356 g/mole for MAG and 282 g/mole for FFA.

25

26 *5.3.6 Calculation of the lipolysis level*

1 The lipolysis level (LL%) corresponding to the percentage of the total meal TAG (TAG_0) acyl
2 chains converted into "intestinally absorbable" acyl chains, *i.e.* FFA and MAG, was defined by
3 the following equation, where TAG_t , DAG_t , MAG_t and FFA_t are the amounts (in mmol) of
4 residual triacylglycerols and lipolysis products recovered at a given time t during the hydrolysis
5 process:

$$6 \quad \text{LL\%} = 100 \times (\text{MAG}_t + \text{FFA}_t) / (3 \times \text{TAG}_t + 2 \times \text{DAG}_t + \text{MAG}_t + \text{FFA}_t)$$
$$7 \quad = 100 \times (\text{MAG}_t + \text{FFA}_t) / (3 \times \text{TAG}_0)$$

8

9 5.4 Animals, surgical procedures and lymph analysis

10 5.4.1 Lipid emulsion preparation

11 Oil-in-water (O/W) emulsions were prepared at room temperature. The oil phase contained 1 g
12 of sodium deoxycholate (Sigma-Aldrich-Fluka Chimie, St-Quentin-Fallavier, France) and 20 g
13 of Lipoid PC (Lipoid[®] from Lipoid AG, Sennweidstrasse / ZG, Switzerland) per 100 g of olive
14 oil (Huile d'olive vierge extra Bio - Carrefour). The oil phase was manually dispersed into the
15 aqueous phase to an oil fraction of 45 g per 100 g. The coarse O/W emulsions obtained were
16 then sheared using an Ultraturax apparatus (IKA, Staufen, Germany), equipped with a generator
17 axis (10 mm S25-N-10G; IKA, Staufen, Germany) under a nitrogen flux to prevent lipid
18 oxidation. Based on previous *in vivo* studies conducted with **Orlistat** on fat absorption in rats
19 [70-72], each inhibitor was first premixed with the olive oil emulsion and administered to rats
20 at a dose of 5.3 mg/kg of body weight (*i.e.*, 3.21 µmol of **Orlistat** or 3.96 µmol of **BemPPOX**).

21

22 5.4.2 Animals and surgical procedures

23 Male Wistar rats (8 weeks old, body weight 300-350 g) were obtained from Elevage Janvier
24 (St-Berthevin, France) and were randomly assigned to one of the three groups (*Control*, **Orlistat**
25 and **BemPPOX** groups). The study was conducted in accordance with European Community
26 Council Directives 2010/63/EU for animal experiments. All experiments conformed to the

1 Guidelines for the Handling and Training of Laboratory Animals. Rats were housed for at least
2 3 days before the experiment in a controlled environment, with constant temperature and
3 humidity, and with free water and food access.
4 Rats were fed a fat-free diet (Epinay, France) and had free access to water 24 h before the
5 surgery. For collecting the lymph, a polyethylene catheter (inner diameter 0.86 mm, outer
6 diameter 1.27 mm; Biotrol, Paris, France) was inserted into the main mesenteric lymph duct of
7 each rat placed under ketamine/xylazine anesthesia (100 and 10 mg/g of body weight,
8 respectively), as described previously [26, 27, 89, 90]. After the surgery, rats were placed in
9 individual restraining cages, in a warm environment, with tap water freely available.
10 A few hours later, 0.8 mL of olive oil emulsion, corresponding to a total amount of 530 mg
11 fatty acids per rat, in presence or not of inhibitory compounds, were directly provided in the
12 mouth of rats, followed by 0.5 mL of water. The study was performed on 7 cannulated rats for
13 each group: the “*Control group*” received only olive oil emulsion, while the two others received
14 olive oil emulsion supplemented with **Orlistat** and **BemPPOX**, respectively. Lymph was
15 collected over a 24-h period with fractionation in glass tubes maintained in an ice bath and
16 stored at -80 °C until analysis. During the collection period, the lymph flow averaged 0.30
17 (SEM 0.03) mL/h.

18

19 5.4.3 Analysis of lymph lipids

20 Lipids from lymph samples were trans-methylated according to the method of Lepage & Roy
21 [91]. Heptadecanoic acid (C17:0) was added as an internal standard for TAG fatty acid
22 quantification. Fatty acid methyl esters were analyzed by gas chromatography on a BPX 70
23 capillary column (60 m long, 0.25 mm film, 0.25 mm inner diameter - SGE, Victoria, Australia
24 - H₂ as a carrier gas and split ratio of 1:80). The gas chromatograph (Focus GC;
25 Thermofinnigan, Courtaboeuf, France) was equipped with a flame ionization detector
26 maintained at 280 °C. The injector temperature was 250 °C. The column temperature was

1 increased from 150 to 200 °C (1.3 °C/min), maintained at 200 °C for 20 min, increased from
2 200 to 235 °C (10 °C/min) and held at 235 °C for 20 min. Data handling was performed using
3 Chromquest software (Thermofinnigan, Courtaboeuf, France). Methylated fatty acid mixtures
4 (Sigma, St Quentin Fallavier, France) and natural extracts of known composition were used as
5 standards for column calibration. The variation in peak area between injections was less than
6 2%.

7

8 *5.4.5 Statistical analysis*

9 Data are expressed as means ± standard errors (SD). The area under the curve was calculated
10 according to the trapezoidal method [92]. The statistical significance of differences in the
11 lymphatic total fatty acid concentrations between the three group conditions (*Control*, *Orlistat*
12 and *BemPPOX* groups) was analyzed by one-way ANOVA followed by a post hoc Fisher's
13 test. Only the above tests with *p-value* < 0.05 were judged to be significant.

14

1 **Acknowledgements**

2 Financial supports from the Agence Nationale de la Recherche (ANR PCV 2007-184840
3 PHELIN), the LISA Carnot Institute (ANR n°07-CARN-009-01), the Ministère de
4 l'Enseignement Supérieur et de la Recherche (AB, BR) and CNRS are acknowledged.

5

6

7 **Supplementary data**

8 Supplementary data associated with this article can be found in the online version.

9 These data include half-inactivation time ($t_{1/2}$) and x_{150} values of **BemPPOX** and **Orlistat**
10 measured on digestive lipases (**Table S1**); *in silico* molecular docking experiments on GPLRP2
11 and hCEH (**Figs. S2 & S3**); and the spectral data (^1H & ^{13}C NMR spectra, HRMS spectrum) of
12 each new oxadiazolone compound (**Figs. S4-S16**).

13

1 **REFERENCES**
2

- 3 [1] G.A. Bray, Medical consequences of obesity, *J Clin Endocrinol Metab*, 89 (2004) 2583-2589.
- 4 [2] F. Carrière, C. Renou, S. Ransac, V. Lopez, J. De Caro, F. Ferrato, A. De Caro, A. Fleury, P.
5 Sanwald-Ducray, H. Lengsfeld, C. Beglinger, P. Hadvary, R. Verger, R. Laugier, Inhibition of
6 gastrointestinal lipolysis by Orlistat during digestion of test meals in healthy volunteers, *Am J Physiol
7 Gastrointest Liver Physiol*, 281 (2001) G16-28.
- 8 [3] L. Sjöström, A. Rissanen, T. Andersen, M. Boldrin, A. Golay, H.P.F. Koppeschaar, M. Krempf,
9 Randomised placebo-controlled trial of orlistat for weight loss and prevention of weight regain in obese
10 patients, *The Lancet*, 352 (1998) 167-172.
- 11 [4] A. Ballinger, S. Peikin, Orlistat: its current status as an anti-obesity drug, *Eur J Pharmacol*, 440
12 (2002) 109-117.
- 13 [5] W.H. Saris, Very-low-calorie diets and sustained weight loss, *Obes Res*, 9 Suppl 4 (2001) 295S-
14 301S.
- 15 [6] A.G. Tsai, T.A. Wadden, The evolution of very-low-calorie diets: an update and meta-analysis,
16 *Obesity (Silver Spring)*, 14 (2006) 1283-1293.
- 17 [7] E. Hemmingsson, K. Johansson, J. Eriksson, J. Sundstrom, M. Neovius, C. Marcus, Weight loss and
18 dropout during a commercial weight-loss program including a very-low-calorie diet, a low-calorie diet,
19 or restricted normal food: observational cohort study, *Am J Clin Nutr*, 96 (2012) 953-961.
- 20 [8] L. Ioannides-Demos, L. Piccenna, J. McNeil, Pharmacotherapies for obesity: past, current, and future
21 therapies, *J Obes.*, ID 179674 (2011).
- 22 [9] K.G. Murphy, S.R. Bloom, Gut hormones and the regulation of energy homeostasis, *Nature*, 444
23 (2006) 854-859.
- 24 [10] K. Suzuki, C.N. Jayasena, S.R. Bloom, The gut hormones in appetite regulation, *J Obes.*, ID 528401
25 (2011).
- 26 [11] P. Hildebrand, C. Petrig, B. Burckhardt, S. Ketterer, H. Lengsfeld, A. Fleury, P. Hadvary, C.
27 Beglinger, Hydrolysis of dietary fat by pancreatic lipase stimulates cholecystokinin release,
28 *Gastroenterology*, 114 (1998) 123-129.
- 29 [12] G.J. Dockray, Gastrointestinal hormones and the dialogue between gut and brain, *The Journal of
30 Physiology*, 592 (2014) 2927-2941.
- 31 [13] M. Ellrichmann, M. Kapelle, P.R. Ritter, J.J. Holst, K.H. Herzig, W.E. Schmidt, F. Schmitz, J.J.
32 Meier, Orlistat inhibition of intestinal lipase acutely increases appetite and attenuates postprandial
33 glucagon-like peptide-1-(7-36)-amide-1, cholecystokinin, and peptide YY concentrations, *J Clin
34 Endocrinol Metab*, 93 (2008) 3995-3998.

- 1 [14] P.W. Maljaars, H.P. Peters, D.J. Mela, A.A. Masclee, Ileal brake: a sensible food target for appetite
2 control. A review, *Physiol. Behav.*, 95 (2008) 271-281.
- 3 [15] F. Carrière, J.A. Barrowman, R. Verger, R. Laugier, Secretion and contribution to lipolysis of
4 gastric and pancreatic lipases during a test meal in humans, *Gastroenterology*, 105 (1993) 876-888.
- 5 [16] H. Lengsfeld, G. Beaumier-Gallon, H. Chahinian, A. De Caro, R. Verger, R. Laugier, F. Carrière,
6 Physiology of Gastrointestinal Lipolysis and Therapeutical Use of Lipases and Digestive Lipase
7 Inhibitors, in: G. Müller, and Petry, S. (Ed.) *Lipases and phospholipases in drug development*, Wiley-
8 VCH, Weinheim, 2004, pp. 195-223.
- 9 [17] Y. Gargouri, G. Piéroni, C. Rivière, P.A. Lowe, J.-F. Saunière, L. Sarda, R. Verger, Importance of
10 human gastric lipase for intestinal lipolysis: an *in vitro* study, *Biochim Biophys. Acta*, 879 (1986) 419-
11 423.
- 12 [18] S. Bernbäck, L. Bläckberg, O. Hernell, Fatty acids generated by gastric lipase promote human milk
13 triacylglycerol digestion by pancreatic colipase-dependent lipase, *Biochim Biophys. Acta*, 1001 (1989)
14 286-291.
- 15 [19] S. Bernbäck, L. Blackberg, O. Hernell, The complete digestion of milk triacylglycerol *in vitro*
16 requieres gastric lipase, pancreatic colipase-dependant lipase and bile salt-stimulated lipase, *J. Clin.*
17 *Invest.*, 85 (1990) 1221-1226.
- 18 [20] S.B. Clark, B. Brause, P.R. Holt, Lipolysis and absorption of fat in the rat stomach,
19 *Gastroenterology*, 56 (1969) 214-222.
- 20 [21] J.P. Perret, [Gastric lipolysis of maternal milk triglycerides, and gastric absorption of medium chain
21 fatty acids in the young rabbit (author's transl)], *J Physiol.*, 76 (1980) 159-166.
- 22 [22] H.-C. Lai, D.M. Ney, Gastric Digestion Modifies Absorption of Butterfat into Lymph
23 Chylomicrons in Rats, *J Nutr.*, 128 (1998) 2403-2410.
- 24 [23] V. Point, K.V. Pavan Kumar, S. Marc, V. Delorme, G. Parsiegla, S. Amara, F. Carriere, G. Buono,
25 F. Fotiadu, S. Canaan, J. Leclaire, J.-F. Cavalier, Analysis of the discriminative inhibition of mammalian
26 digestive lipases by 3-phenyl substituted 1,3,4-oxadiazol-2(3H)-ones, *Eur J Med Chem*, 58 (2012) 452-
27 463.
- 28 [24] F. Carrière, P. Grandval, C. Renou, A. Palomba, F. Priéri, J. Giallo, F. Henniges, S. Sander-
29 Struckmeier, R. Laugier, Quantitative study of digestive enzyme secretion and gastrointestinal lipolysis
30 in chronic pancreatitis, *Clin. Gastroenterol. Hepatol.*, 3 (2005) 28-38.
- 31 [25] P. Capolino, C. Guérin, J. Paume, J. Giallo, J.-M. Ballester, J.-F. Cavalier, F. Carrière, In Vitro
32 Gastrointestinal Lipolysis: Replacement of Human Digestive Lipases by a Combination of Rabbit
33 Gastric and Porcine Pancreatic Extracts, *Food Dig.*, 2 (2011) 43-51.

- 1 [26] L. Couedelo, C. Boue-Vaysse, L. Fonseca, E. Montesinos, S. Djoukitch, N. Combe, M. Cansell,
2 Lymphatic absorption of alpha-linolenic acid in rats fed flaxseed oil-based emulsion, Br. J. Nutr., 105
3 (2011) 1026-1035.
- 4 [27] L. Couedelo, C. Vaysse, E. Vaique, A. Guy, I. Gosse, T. Durand, S. Pinet, M. Cansell, N. Combe,
5 The fraction of alpha-linolenic acid present in the sn-2 position of structured triacylglycerols decreases
6 in lymph chylomicrons and plasma triacylglycerols during the course of lipid absorption in rats, J Nutr,
7 142 (2012) 70-75.
- 8 [28] F. Carrière, H. Moreau, V. Raphel, R. Laugier, C. Benicourt, J.L. Junien, R. Verger, Purification
9 and biochemical characterization of dog gastric lipase, Eur. J. Biochem., 202 (1991) 75-83.
- 10 [29] S. Fernandez, S. Chevrier, N. Ritter, B. Mahler, F. Demarne, F. Carriere, V. Jannin, In vitro
11 gastrointestinal lipolysis of four formulations of piroxicam and cinnarizine with the self emulsifying
12 excipients Labrasol and Gelucire 44/14, Pharm. Res., 26 (2009) 1901-1910.
- 13 [30] A. Roussel, N. Miled, L. Berti-Dupuis, M. Riviere, S. Spinelli, P. Berna, V. Gruber, R. Verger, C.
14 Cambillau, Crystal structure of the open form of dog gastric lipase in complex with a phosphonate
15 inhibitor, J. Biol. Chem., 277 (2002) 2266-2274.
- 16 [31] F. Carrière, C. Withers-Martinez, H. van Tilburgh, A. Roussel, C. Cambillau, R. Verger, Structural
17 basis for the substrate selectivity of pancreatic lipases and some related proteins., Biochim Biophys.
18 Acta, 1376 (1998) 417-432.
- 19 [32] A. Hjorth, F. Carrière, C. Cudrey, H. Wöldike, E. Boel, D.M. Lawson, F. Ferrato, C. Cambillau,
20 G.G. Dodson, L. Thim, R. Verger, A structural domain (the lid) found in pancreatic lipases is absent in
21 the guinea pig (phospho)lipase, Biochemistry, 32 (1993) 4702-4707.
- 22 [33] C. Withers-Martinez, F. Carrière, R. Verger, D. Bourgeois, C. Cambillau, A pancreatic lipase with
23 a phospholipase A1 activity: crystal structure of a chimeric pancreatic lipase-related protein 2 from
24 guinea pig., Structure, 4 (1996) 1363-1374.
- 25 [34] C. Cudrey, H. van Tilburgh, Y. Gargouri, R. Verger, Inactivation of pancreatic lipases by
26 amphiphilic reagents 5-(Dodecyldithio)-2-nitrobenzoic acid and tetrahydrolipstatin. Dependence upon
27 partitioning between micellar and oil phases, Biochemistry, 32 (1993) 13800-13808.
- 28 [35] S. Ransac, Y. Gargouri, F. Marguet, G. Buono, C. Beglinger, P. Hildebrand, H. Lengsfeld, P.
29 Hadváry, R. Verger, Covalent inactivation of lipases, Methods Enzymol., 286 (1997) 190-231.
- 30 [36] V. Point, R.K. Malla, S. Diomande, B.P. Martin, V. Delorme, F. Carriere, S. Canaan, N.P. Rath,
31 C.D. Spilling, J.-F. Cavalier, Synthesis and kinetic evaluation of cyclophostin and cyclipostins
32 phosphonate analogs as selective and potent inhibitors of microbial lipases, J Med Chem, 55 (2012)
33 10204-10219.

- 1 [37] A. Roussel, Y. Yang, F. Ferrato, R. Verger, C. Cambillau, M. Lowe, Structure and activity of rat
2 pancreatic lipase-related protein 2., *J. Biol. Chem.*, 273 (1998) 32121-32128.
- 3 [38] C. Eydoux, S. Spinelli, T.L. Davis, J.R. Walker, A. Seitova, S. Dhe-Paganon, A. De Caro, C.
4 Cambillau, F. Carriere, Structure of human pancreatic lipase-related protein 2 with the lid in an open
5 conformation, *Biochemistry*, 47 (2008) 9553-9564.
- 6 [39] J. De Caro, B. Sias, P. Grandval, F. Ferrato, H. Halimi, F. Carriere, A. De Caro, Characterization
7 of pancreatic lipase-related protein 2 isolated from human pancreatic juice, *Biochimica et Biophysica
8 Acta (BBA) - Proteins & Proteomics*, 1701 (2004) 89-99.
- 9 [40] C. Eydoux, J. De Caro, F. Ferrato, P. Boullanger, D. Lafont, R. Laugier, F. Carrière, A. De Caro,
10 Further biochemical characterization of human pancreatic lipase-related protein 2 expressed in yeast
11 cells, *J. Lipid Res.*, 48 (2007) 1539-1549.
- 12 [41] S. Amara, N. Barouh, J. Lecomte, D. Lafont, S. Robert, P. Villeneuve, A. De Caro, F. Carrière,
13 Lipolysis of natural long chain and synthetic medium chain galactolipids by pancreatic lipase-related
14 protein 2, *Biochimica et Biophysica Acta (BBA) - Molecular and Cell Biology of Lipids*, 1801 (2010)
15 508-516.
- 16 [42] D. Lombardo, O. Guy, C. Figarella, Purification and characterization of a carboxyl ester hydrolase
17 from human pancreatic juice, *Biochim Biophys. Acta*, 527 (1978) 142-149.
- 18 [43] H.L. Brockman, Triglyceride lipase from porcine pancreas., *Methods Enzymol.*, 71 (1981) 619-
19 627.
- 20 [44] O. Guy, C. Figarella, The proteins of human pancreatic external secretion, *Scandinavian Journal of
21 Gastroenterology. Supplement*, 67 (1981) 59-61.
- 22 [45] E.A. Rudd, H.L. Brockman, Pancreatic carboxyl ester lipase (cholesterol esterase), in: B.
23 Borgström, H.L. Brockman (Eds.) *Lipases*, Elsevier Science Publishers, Amsterdam, 1984, pp. 185-204.
- 24 [46] J.-C. Bakala N'Goma, S. Amara, K. Dridi, V. Jannin, F. Carrière, Understanding the lipid-digestion
25 processes in the GI tract before designing lipid-based drug-delivery systems, *Ther Deliv.*, 3 (2011) 105-
26 124.
- 27 [47] S. Fernandez, J.-D. Rodier, N. Ritter, B. Mahler, F. Demarne, F. Carrière, V. Jannin, Lipolysis of
28 the semi-solid self-emulsifying excipient Gelucire® 44/14 by digestive lipases, *Biochim Biophys. Acta*,
29 1781 (2008) 367-375.
- 30 [48] Y. Ben Ali, R. Verger, F. Carrière, S. Petry, G. Muller, A. Abousalham, The molecular mechanism
31 of human hormone-sensitive lipase inhibition by substituted 3-phenyl-5-alkoxy-1,3,4-oxadiazol-2-ones,
32 *Biochimie*, 94 (2012) 137-145.

- 1 [49] A. Roussel, S. Canaan, M.P. Egloff, M. Rivière, L. Dupuis, R. Verger, C. Cambillau, Crystal
2 structure of Human gastric lipase and model of lysosomal acid lipase, two lipolytic enzymes of medical
3 interest, *J. Biol. Chem.*, 274 (1999) 16995-17002.
- 4 [50] S. Terzyan, C.S. Wang, D. Downs, B. Hunter, X.C. Zhang, Crystal structure of the catalytic domain
5 of human bile salt activated lipase, *Protein Science*, 9 (2000) 1783-1790.
- 6 [51] R.A. Laskowski, M.B. Swindells, LigPlot+: Multiple Ligand–Protein Interaction Diagrams for
7 Drug Discovery, *Journal of Chemical Information and Modeling*, 51 (2011) 2778-2786.
- 8 [52] F. Carrière, C. Renou, V. Lopez, J. De Caro, F. Ferrato, H. Lengsfeld, A. De Caro, R. Laugier , R.
9 Verger, The Specific Activities of Human Digestive Lipases Measured From the In Vivo and In Vitro
10 Lipolysis of Test Meals, *Gastroenterology*, 119 (2000) 949-960.
- 11 [53] J.-C. Bakala-N'Goma, H. Williams, P. Sassene, K. Kleberg, M. Calderone, V. Jannin, A. Igonin,
12 A. Partheil, D. Marchaud, E. Jule, J. Vertommen, M. Maio, R. Blundell, H. Benamer, A. Müllertz, C.
13 Pouton, C.H. Porter, F. Carrière, Toward the Establishment of Standardized In Vitro Tests for Lipid-
14 Based Formulations. 5. Lipolysis of Representative Formulations by Gastric Lipase, *Pharm Res.*, 32
15 (2015) 1279-1287.
- 16 [54] C. Vors, P. Capolino, C. Guerin, E. Meugnier, S. Pesenti, M.A. Chauvin, J. Monteil, N. Peretti, M.
17 Cansell, F. Carriere, M.C. Michalski, Coupling in vitro gastrointestinal lipolysis and Caco-2 cell cultures
18 for testing the absorption of different food emulsions, *Food Funct*, 3 (2012) 537-546.
- 19 [55] L. Couedelo, S. Amara, M. Lecomte, E. Meugnier, J. Monteil, L. Fonseca, G. Pineau, M. Cansell,
20 F. Carriere, M.C. Michalski, C. Vaysse, Impact of various emulsifiers on ALA bioavailability and
21 chylomicron synthesis through changes in gastrointestinal lipolysis, *Food Funct*, 6 (2015) 1726-1735.
- 22 [56] J.O. Christensen, K. Schultz, B. Mollgaard, H.G. Kristensen, A. Mullertz, Solubilisation of poorly
23 water-soluble drugs during in vitro lipolysis of medium- and long-chain triacylglycerols, *Eur J Pharm
Sci*, 23 (2004) 287-296.
- 25 [57] C.J. Porter, A.M. Kaukonen, A. Taillardat-Bertschinger, B.J. Boyd, J.M. O'Connor, G.A. Edwards,
26 W.N. Charman, Use of in vitro lipid digestion data to explain the in vivo performance of triglyceride-
27 based oral lipid formulations of poorly water-soluble drugs: studies with halofantrine, *J Pharm Sci*, 93
28 (2004) 1110-1121.
- 29 [58] S. Abdelkafi, B. Fouquet, N. Barouh, S. Durner, M. Pina, F. Scheirlinckx, P. Villeneuve, F.
30 Carrière, In vitro comparisons between *Carica papaya* and pancreatic lipases during test meal lipolysis:
31 potential use of CPL in enzyme replacement therapy, *Food Chem.*, 115 (2009) 488-494.
- 32 [59] A. Sarkar, D.S. Horne, H. Singh, Pancreatin-induced coalescence of oil-in-water emulsions in an
33 in vitro duodenal model, *International Dairy Journal*, 20 (2010) 589-597.

- 1 [60] J.-F. Cavalier, D. Lafont, P. Boullanger, D. Houisse, J. Giallo, J.-M. Ballester, F. Carrière,
2 Validation of lipolysis product extraction from aqueous/biological samples, separation and
3 quantification by thin-layer chromatography with flame ionization detection analysis using O-
4 cholestryl ethylene glycol as a new internal standard, *J. Chromatogr. A*, 1216 (2009) 6543-6548.
- 5 [61] G. Benzonana, P. Desnuelle, [Kinetic study of the action of pancreatic lipase on emulsified
6 triglycerides. Enzymology assay in heterogeneous medium], *Biochim Biophys. Acta*, 105 (1965) 121-
7 136.
- 8 [62] M. Armand, B. Pasquier, P. Borel, M. Andre, M. Senft, J. Peyrot, J. Salducci, D. Lairon, Emulsion
9 and absorption of lipids: the importance of physicochemical properties, *OCL. Oléagineux, corps gras,*
10 *lipides*, 4 (1997) 178-185.
- 11 [63] M. Golding, T.J. Wooster, The influence of emulsion structure and stability on lipid digestion,
12 *Current Opinion in Colloid & Interface Science*, 15 (2010) 90-101.
- 13 [64] P.M. Reis, T.W. Raab, J.Y. Chuat, M.E. Leser, R. Miller, H.J. Watzke, K. Holmberg, Influence of
14 Surfactants on Lipase Fat Digestion in a Model Gastro-intestinal System, *Food Biophys.*, 3 (2008) 370-
15 381.
- 16 [65] V. Delorme, R. Dhouib, S. Canaan, F. Fotiadu, F. Carrière, J.-F. Cavalier, Effects of Surfactants on
17 Lipase Structure, Activity and Inhibition, *Pharm. Res.*, 28 (2011) 1831-1842.
- 18 [66] S.J. DeNigris, M. Hamosh, D.K. Kasbekar, T.C. Lee, P. Hamosh, Lingual and gastric lipases :
19 species differences in the origin of prepancreatic digestive lipases and in the localization of gastric
20 lipase, *Biochimica et Biophysica Acta (BBA) - Proteins & Proteomics*, 959 (1988) 38-45.
- 21 [67] M. Hamosh, D. Ganot, P. Hamosh, Rat lingual lipase : Characteristics of enzyme activity, *J. Biol.*
22 *Chem.*, 254 (1979) 12121-12125.
- 23 [68] A.J.P. Docherty, M.W. Bodmer, S. Angal, R. Verger, C. Rivière, P.A. Lowe, A. Lyons, J.S. Emtage,
24 T.J.R. Harris, Molecular cloning and nucleotide sequence of rat lingual lipase cDNA, *Nucleic Acid Res.*,
25 13 (1985) 1891-1903.
- 26 [69] M.W. Bodmer, S. Angal, G.T. Yarranton, T.J.R. Harris, A. Lyons, D.J. King, G. Piéroni, C. Rivière,
27 R. Verger, P.A. Lowe, Molecular cloning of a human gastric lipase and expression of the enzyme in
28 yeast, *Biochim Biophys. Acta*, 909 (1987) 237-244.
- 29 [70] D. Isler, C. Moeglen, N. Gains, M.K. Meier, Effect of the lipase inhibitor orlistat and of dietary
30 lipid on the absorption of radiolabelled triolein, tri-gamma-linolenin and tripalmitin in mice, *The British*
31 *journal of nutrition*, 73 (1995) 851-862.
- 32 [71] E. Fernandez, B. Borgstrom, Effects of tetrahydrolipstatin, a lipase inhibitor, on absorption of fat
33 from the intestine of the rat, *Biochim Biophys. Acta*, 1001 (1989) 249-255.

- 1 [72] T. Porsgaard, E.M. Straarup, H. Mu, C.E. Høy, Effect of orlistat on fat absorption in rats: A
2 comparison of normal rats and rats with diverted bile and pancreatic juice, *Lipids*, 38 (2003) 1039-1043.
- 3 [73] D. Perrin, W. Armarego, D.R. Perrin, *Purification of Laboratory Chemicals*, 2nd Ed, Pergamon
4 Press, Oxford, 1980.
- 5 [74] W.C. Still, M. Kahn, A. Mitra, Rapid chromatographic technique for preparative separation with
6 moderate resolution, *J. Org. Chem.*, 43 (1978) 2923-2925.
- 7 [75] V. Gruber, P. Berna, T. Arnaud, P. Bournat, C. Clément, D. Mison, B. Olagnier, L. Philippe, M.
8 Theisen, S. Baudino, Large-scale production of a therapeutic protein in transgenic tobacco plants: effect
9 of subcellular targeting on quality of a recombinant dog gastric lipase, *Molecular Breeding*, 7 (2001)
10 329-340.
- 11 [76] E. Mas, N. Abouakil, S. Roudani, J.L. Franc, J. Montreuil, D. Lombardo, Variation of the
12 glycosylation of human pancreatic bile-salt-dependent lipase., *Eur. J. Biochem.*, 216 (1993) 807-812.
- 13 [77] J. De Caro, F. Carrière, P. Barboni, T. Giller, R. Verger, A. De Caro, Pancreatic lipase-related
14 protein 1 (PLRP1) is present in the pancreatic juice of several species., *Biochim Biophys. Acta*, 1387
15 (1998) 331-341.
- 16 [78] R. Field, R.O. Scow, Purification and characterization of rat lingual lipase, *J. Biol. Chem.*, 258
17 (1983) 14563-14569.
- 18 [79] C. Erlanson, B. Borgstrom, Tributyrine as a substrate for determination of lipase activity of
19 pancreatic juice and small intestinal content., *Scandinavian Journal of Gastroenterology. Supplement*, 5
20 (1970) 293-295.
- 21 [80] Y. Gargouri, G. Piéroni, C. Rivière, J.-F. Saunière, P.A. Lowe, L. Sarda, R. Verger, Kinetic assay
22 of human gastric lipase on short- and long-chain triacylglycerol emulsions, *Gastroenterology*, 91 (1986)
23 919-925.
- 24 [81] S. Amara, D. Lafont, B. Fiorentino, P. Boullanger, F. Carrière, A. De Caro, Continuous
25 measurement of galactolipid hydrolysis by pancreatic lipolytic enzymes using the pH-stat technique and
26 a medium chain monogalactosyl diglyceride as substrate, *Biochimica et Biophysica Acta (BBA)* -
27 *Proteins & Proteomics*, 1791 (2009) 983-990.
- 28 [82] F. Marguet, C. Cudrey, R. Verger, G. Buono, Digestive lipases: Inactivation by phosphonates,
29 *Biochim Biophys. Acta*, 1210 (1994) 157-166.
- 30 [83] V. Belle, A. Fournel, M. Woudstra, S. Ranaldi, F. Prieri, V. Thome, J. Currault, R. Verger, B.
31 Guigliarelli, F. Carriere, Probing the Opening of the Pancreatic Lipase Lid Using Site-Directed Spin
32 Labeling and EPR Spectroscopy, *Biochemistry*, 46 (2007) 2205-2214.

- 1 [84] M. Rouard, H. Sari, S. Nurit, B. Entressangles, P. Desnuelle, Inhibition of pancreatic lipase by
2 mixed micelles of diethyl *p*-nitrophenyl phosphate and the bile salts, Biochimica et Biophysica Acta
3 (BBA) - Proteins & Proteomics, 530 (1978) 227-235.
- 4 [85] M.L.M. Mannesse, J.W.P. Boots, R. Dijkman, A.J. Slotboom, H.T.W.V. Vanderhijden, M.R.
5 Egmond, H.M. Verheij, G.H. Dehaas, Phosphonate analogues of triacylglycerols are potent inhibitors
6 of lipase, Biochim Biophys. Acta, 1259 (1995) 56-64.
- 7 [86] O. Trott, A.J. Olson, AutoDock Vina: Improving the speed and accuracy of docking with a new
8 scoring function, efficient optimization, and multithreading, Journal of Computational Chemistry, 31
9 (2010) 455-461.
- 10 [87] D. Seeliger, B.L. de Groot, Ligand docking and binding site analysis with PyMOL and
11 Autodock/Vina, J. Comput. Aided Mol. Des., 24 (2010) 417-422.
- 12 [88] J. Folch, M. Lees, G.H. Sloane Stanley, A simple method for the isolation and purification of total
13 lipids from animal tissues, J. Biol. Chem., 226 (1957) 497-509.
- 14 [89] J.L. Bollman, J.C. Cain, J.H. Grindlay, Techniques for the collection of lymph from the liver, small
15 intestine, or thoracic duct of the rat, J Lab Clin Med, 33 (1948) 1349-1352.
- 16 [90] N. Combe, M.J. Constantin, B. Entressangles, Lymphatic absorption of nonvolatile oxidation
17 products of heated oils in the rat, Lipids, 16 (1981) 8-14.
- 18 [91] G. Lepage, C.C. Roy, Improved recovery of fatty acid through direct transesterification without
19 prior extraction or purification, J Lipid Res., 25 (1984) 1391-1396.
- 20 [92] G. Dahlquist, Å. Björck, Numerical Integration, in: Numerical Methods in Scientific Computing,
21 Volume I, SIAM, Philadelphia, 2008, pp. 521-607.
- 22
- 23

1 **Table 1.** Inhibition of DGL, GPLRP2, and pancreatic lipase contained in PPE or HPJ after a 30-min incubation period with each **RmPPOX** inhibitor.^a

Compounds	DGL			GPLRP2			PPE		HPJ	
	%inhibition		$x_I = 4$	%inhibition		$x_I = 400$	x_{I50}	%inhibition		$x_I = 400$
	$x_I = 4$	$x_I = 20$		$x_I = 4$	$x_I = 20$			x_{I50}		
MmPPOX ^b	30.1	81.9	8.33	82.3	88.5	0.77	89.7	~101	49.1 (42.7) ^c	>400
MpPPOX ^b	27.7	92.7	7.12	14.3	31.5	>40	90.6	ND	25.6 (20.0) ^c	>400
MPOX ^b	2.5	6.6	>40	81.9	82.7	0.74	34.1	>400	4.0 (NI) ^c	>400
EmPPOX	33.6	83.0	6.08	27.4	27.7	>40	19.0	>400	18.8	>400
BmPPOX	41.5	77.5	5.33	42.4	43.8	>40	19.7	>400	19.1	>400
iBmPPOX	35.2	69.6	5.51	73.6	76.0	0.52	20.6	>400	21.2	>400
HmPPOX	43.5	65.9	4.92	90.7	91.3	1.09	27.2	>400	17.1	>400
OmPPOX	53.9	70.5	3.99	62.3	63.0	1.47	19.9	>400	25.7	>400
EhmPPOX	14.6	37.7	>100	56.4	57.4	2.72	32.5	>400	20.1	>400
DmPPOX	44.1	68.2	4.57	53.1	54.4	1.17	27.9	>400	29.1	>400
DomPPOX	21.6	27.6	>100	47.9	54.8	2.80	18.9	>400	22.4	>400
BemPPOX	87.6	91.5	0.50	60.6	62.7	0.64	13.2	>400	19.3	>400
MemPPOX	18.1	69.1	11.8	60.3	61.8	1.70	15.5	>400	20.0	>400
Orlistat ^b	53.6	56.3	5.60	85.9	82.4	0.53	93.1	1.35	91.5	11.1

2 ^a Inhibition data (% of initial activity), at inhibitor molar excess (x_I) of 4, 20 or 400 related to 1 mole of enzyme. Values are means of at least three independent assays
3 (CV% < 5.0%). The inhibitor molar excess leading to 50% lipase inhibition, x_{I50} , was determined as described in **Experimental Section**. ND = not determined. NI =
4 no inhibition. ^b Data on DGL and GPLRP2 are from [23]. ^c Numbers in brackets: percentage of inhibition with pure HPL, from [23].

1

2 **Table 2:** Effect of **BemPPOX** and **Orlistat** on the lipolysis of test meals under *in vitro* conditions mimicking the gastric and duodenal phases of digestion.^a

Meal	Treatment	Inhibition (%)		Lipolysis level (LL%)^b		
		DGL <i>t</i> = 29 min	PPE <i>t</i> = 90 min	<i>t</i> = 29 min	<i>t</i> = 45 min	<i>t</i> = 90 min
Liquid Meal: <i>Ensure Plus</i>	Control	-	-	22.3 ± 1.4 (100)	58.0 ± 3.1 (100)	63.6 ± 2.6 (100)
	Orlistat	100	86.6 ± 5.4	0.0 (0)	9.1 ± 0.49 (15.6)	14.4 ± 0.72 (22.6)
	BemPPOX	100	5.6 ± 0.28	4.5 ± 0.22 (20.2)	48.1 ± 1.8 (82.9)	55.3 ± 2.6 (86.9)
Solid meal: beef, fries, butter, oil	Control	-	-	13.0 ± 1.2 (100)	24.7 ± 0.87 (100)	45.4 ± 1.4 (100)
	Orlistat	100	85.2 ± 2.1	2.1 ± 0.37 (16.2)	3.0 ± 1.33 (12.3)	9.2 ± 0.61 (20.3)
	BemPPOX	97.2 ± 0.50	5.1 ± 0.10	3.1 ± 0.22 (23.8)	20.6 ± 1.2 (83.3)	33.7 ± 2.5 (74.2)

3

4 ^aResults are expressed as mean values ± SD (*n* = 3; CV% < 10.0%). ^bLipolysis levels are expressed in % of total meal triacylglycerol fatty acids converted into FFA
5 and MAG. Numbers in brackets: percentage of respective control values.

6

1

2 **Table 3.** Post-prandial levels of fatty acids from lymph TAG in rats fed with olive oil emulsion in the
 3 absence/presence of **Orlistat** or **BemPPOX**. V_i , initial velocity of fatty acid output; C_{max} , maximum fatty acid
 4 concentration; T_{max} , time required to reach C_{max} ; AUC, area under the curve.^a

	V_i (mg/mL/h)	C_{max} (mg/mL)	T_{max} (h)	AUC (h × mg/mL)	
				$t = 6$ h	$t = 24$ h
Control group	12.3 ± 0.46 †	48.5 ± 3.6 †	6	132.0 ± 16.7 †	645.4 ± 68.0 †
Orlistat group	4.4 ± 0.25 ‡	22.9 ± 3.0 ‡	6	82.6 ± 7.6 ‡	187.7 ± 32.5 ‡
BemPPOX group	9.8 ± 0.32 ⊥	33.6 ± 4.3 ⊥	5-8	120.1 ± 9.7 †	490.2 ± 48.0 ⊥

5 ^a Results are expressed as mean values ± standard error of the mean (SEM, $n = 7$ rats per group). Mean values in
 6 a row with superscripts (†, ‡, ⊥) without a common symbol differ significantly (p -value < 0.05; ANOVA
 7 followed by Fisher's test).

9

10

11